

I. EFFECTS OF ADENINE NUCLEOTIDES ON THE CATALYTIC
ACTIVITY OF MITOCHONDRIAL PORCINE HEART MALATE
DEHYDROGENASE II. LIGAND INDUCED CONFOR-
MATIONAL TRANSITIONS AND SECONDARY
STRUCTURE COMPONENTS OF CHICKEN
LIVER PYRUVATE CARBOXYLASE

By

KAREN SUE REINSCHMIEDT MCGURK

Bachelor of Science

Southwestern Oklahoma State University

Weatherford, Oklahoma

1972

Submitted to the Faculty of the Graduate College
of the Oklahoma State University
in partial fulfillment of the requirements
for the Degree of
DOCTOR OF PHILOSOPHY
May, 1976

Thesis
1976D
M148e
Cop. 2



I. EFFECTS OF ADENINE NUCLEOTIDES ON THE CATALYTIC
ACTIVITY OF MITOCHONDRIAL PORCINE HEART MALATE
DEHYDROGENASE II. LIGAND INDUCED CONFOR-
MATIONAL TRANSITIONS AND SECONDARY
STRUCTURE COMPONENTS OF CHICKEN
LIVER PYRUVATE CARBOXYLASE

Thesis Approved:

H. Chris Spivey

Thesis Adviser

Stuart E. Schupp

Chairman Advisory Committee

E. J. Eisenbaum

[Signature]

N. N. Durham

Dean of the Graduate College

964209

ACKNOWLEDGEMENTS

The author would like to extend appreciation to her research adviser, Dr. H. O. Spivey, for advice, guidance, and financial support throughout the completion of work for this thesis. In addition, gratitude is expressed to Drs. S. E. Scheppele, G. J. Mains, and E. J. Eisenbraun, as advisory committee members, and to the chemistry and biochemistry faculties. Appreciation is also extended to Chester North and Dr. R. E. Thompson for their thoughtful help and advice with biochemical techniques and curve fitting methods as well as for their friendship. Gratitude is also expressed to Dr. J. P. Chandler of the Computer Science Department for data analysis advice.

The author also extends appreciation to her parents, John and Lillian Reinschmiedt, for giving her the time, patient understanding, and belief that no goal is unattainable with faith and personal discipline.

To her husband, Donald McGurk, goes special thanks for giving his wife the freedom and encouragement necessary to complete this degree and for setting an example of dedication to science and the education of others in that science. Gratitude is also extended to my sisters and John and Lela McGurk for their encouragement.

Finally, the author gives thanks to her God for protecting her on over 300 trips between Stillwater and Weatherford and for giving her the intellectual ability, endurance, and personal discipline necessary to accomplish her goal.

TABLE OF CONTENTS

Chapter	Page
PART ONE	
I. INTRODUCTION	2
Selected Properties of Malate Dehydrogenase	2
The Effects of Adenine Nucleotides	3
II. EXPERIMENTAL	10
Materials	10
Methods	10
Miscellaneous Reagent Preparations	10
Criteria of Enzyme Purity	11
Enzyme Preparation and Assay	12
Instrumentation	13
Data Analysis	14
III. RESULTS AND DISCUSSION	16
Criteria of Enzyme Purity	16
Ionic Effects	19
ATP and MgATP Inhibition Studies	22
Identification of Factors Altering Enzyme's Kinetic Properties	39
Enzyme Concentration	39
Studies in Potassium Phosphate Buffer	39
Studies in Tris Buffers	42
Buffer Components	45
IV. SUMMARY AND CONCLUSION	49
A SELECTED BIBLIOGRAPHY	50
PART TWO	
I. INTRODUCTION	54
Selected Properties of Pyruvate Carboxylase	54
Ligand Induced Conformational Transitions	56
Secondary Structure Determination by Circular Dichroism	58

TABLE OF CONTENTS (Continued)

Chapter	Page
II. EXPERIMENTAL	60
Materials	60
Methods	60
Miscellaneous Reagent Preparations	60
Enzyme Preparation, Assay, and Protein Determination	62
Pyruvate Carboxylase-ANS Fluorescence Studies	63
Instrumentation	64
Data Analysis	65
III. RESULTS AND DISCUSSION	67
Fluorescence Probe Studies with ϵ -ATP and ϵ -Acetyl-CoA	67
Enzyme Stability and Catalytic Activity Studies at Varying pH's	68
Equilibrium Pyruvate Carboxylase-ANS Fluorescence Studies	69
Dissociation Constant Determination for Enzyme-ANS Complex	75
Effect of ANS on Pyruvate Carboxylase Activity	83
Kinetics of Pyruvate Carboxylase-ANS Binding	83
Kinetics of Ligand Induced Pyruvate Carboxylase-ANS Fluorescence Changes	84
Changes in Circular Dichroism of Pyruvate Carboxylase Induced by ANS, MgATP, and Acetyl-CoA	96
Secondary Structure Estimation Utilizing Far Ultraviolet Circular Dichroism	104
IV. SUMMARY AND CONCLUSION	105
A SELECTED BIBLIOGRAPHY	106
APPENDIXES	108
APPENDIX A - KINETIC TREATMENT OF MECHANISM PROPOSED FOR REACTION OF PYRUVATE CARBOXYLASE-ANS WITH MgATP.	109
APPENDIX B - NOMENCLATURE FOR ENZYME MECHANISMS	117

LIST OF TABLES

Table	Page
PART ONE	
I. Dependence of Specific Activity on Presence of Ions	23
II. Concentrations of Mg ²⁺ Complexed Species and Free Ligands in Phosphate Buffer System as a Function of ATP Concentration	28
III. Results of Regression Analysis of Initial Velocity Data . .	38
IV. Dependence of Specific Activity on Enzyme Concentration at High and Low Substrate Levels	41
V. Effects of Buffer System Components on Enzyme Behavior in the Presence of ATP	46
PART TWO	
I. Dependence of Fluorescence of Pyruvate Carboxylase-ANS Complex on Presence and Order of Addition of Acetyl-CoA, ATP, and KHCO ₃	76
II. Stopped-Flow Kinetics Measurements	85
III. Kinetic Best Fit Values of Equation (3-2) Parameters for MgATP Induced Changes in Enzyme-ANS Fluorescence	90
IV. Effect of MgATP and Acetyl-CoA on Pyruvate Carboxylase and Pyruvate Carboxylase-ANS 292 nm and 285 nm Circular Dichroism Peaks	102

LIST OF FIGURES

Figure	Page
PART ONE	
1. Fluorescence Spectra of Porcine Heart Mitochondrial Malate Dehydrogenase (Sigma - Lot #54C95702), Tyrosine, and Tryptophan	18
2. Cellulose Acetate Electrophoresis of Pig Heart Malate Dehydrogenase	21
3. Inhibition of Porcine Heart Mitochondrial Malate Dehydrogenase by KCl	26
4. Competitive Inhibition of Porcine Heart Mitochondrial Malate Dehydrogenase by ATP	30
5. Noncompetitive Inhibition of Porcine Heart Mitochondrial Malate Dehydrogenase by ATP	32
6. Competitive Inhibition of Porcine Heart Mitochondrial Malate Dehydrogenase by MgATP	34
7. Noncompetitive Inhibition of Porcine Heart Mitochondrial Malate Dehydrogenase by MgATP	36
PART TWO	
1. pH Optimum Determination	71
2. Fluorescence Spectra of ANS and ANS Bound to Pyruvate Carboxylase	73
3. Effect of Varying ANS Concentrations on the Fluorescence of the Pyruvate Carboxylase-ANS Complex in the Presence and Absence of Acetyl-CoA and MgATP	80
4. Replot of Data of Figure 3, Fluorescence as a Function of Fluorescence/[ANS]	82
5. Progress Curves for the Reaction of Pyruvate Carboxylase-ANS with MgATP for Various Enzyme and MgATP Concentrations	88

LIST OF FIGURES (Continued)

Figure	Page
6. Double Reciprocal Plots of Best Fit Values of A2, A3, and A4 (Amplitude Parameters in Equation (3-2)) as a Function of ATP Concentration	94
7. Near Ultraviolet Pyruvate Carboxylase Circular Dichroism Spectrum	99
8. Far Ultraviolet Pyruvate Carboxylase Circular Dichroism Spectrum	101

LIST OF SYMBOLS AND ABBREVIATIONS

ϵ	- Greek epsilon, indicating absorptivity
σ	- Greek sigma, indicating standard deviation
λ	- Greek lambda, indicating wavelength
β	- Greek beta
θ	- Greek theta, indicating measured ellipticity
Δ	- Greek capital delta, indicating change
χ	- Greek chi
\approx	- Approximately
[]	- Concentration
K_i	- Inhibition constant
K_s, K_m	- Michaelis constant for a substrate (S or M)
V_{max}	- Maximum velocity
I	- Inhibitor
I.U.	- International Unit, μ moles product formed/min
S.A.	- Specific activity, μ moles product formed/(min mg)
NADH	- β -Nicotinamide adenine dinucleotide, reduced form
NAD ⁺	- β -Nicotinamide adenine dinucleotide
OAA	- Oxaloacetate
E	- Enzyme
ATP	- Adenosine 5'-triphosphate
AMP	- Adenosine 5'-phosphate
ADP	- Adenosine 5'-diphosphate

LIST OF SYMBOLS AND ABBREVIATIONS (Continued)

- MgATP - Mg^{2+} salt of ATP
- EDTA - Ethylenediaminetetraacetic acid
- Tris - Tris-(hydroxymethyl)-aminomethane
- AcCoA - Acetyl-CoA
- ANS - 8-Anilino-1-naphthalenesulfonic acid

PART ONE

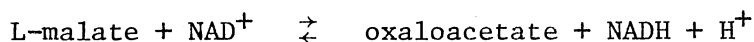
EFFECTS OF ADENINE NUCLEOTIDES ON THE
CATALYTIC ACTIVITY OF MITOCHONDRIAL
PORCINE HEART MALATE
DEHYDROGENASE

CHAPTER I

INTRODUCTION

Selected Properties Of Malate Dehydrogenase

Malate dehydrogenase (EC 1.1.1.37) catalyzes the following reaction.



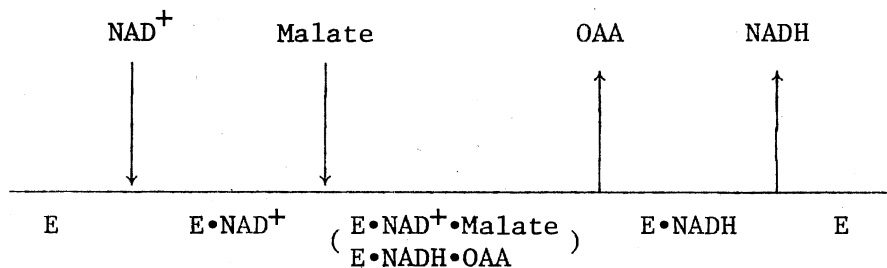
The enzyme occurs in virtually all eukaryotic cells in at least two unique forms identified as mitochondrial (m-MDH) and soluble or cytoplasmic (s-MDH) according to its cellular location (1). The two forms are distinct, differing in amino acid composition, immunologically (2), electrophoretically (3), structurally (4), and catalytically (5).

Malate dehydrogenases have been identified in a wide variety of sources and purified to homogeneity from a number of them. However, the majority of studies have been carried out with enzyme isolated from either pig or beef heart. The mitochondrial porcine heart malate dehydrogenase has a molecular weight of 70,000 (6), is composed of two identical or very similar subunits, and is characterized by its inhibition by oxaloacetate (7) at concentrations above 0.1 mM.

Functionally, the soluble enzyme is generally considered to take part in the cytoplasmic side of the "malate shuttle," providing a means of transporting NADH equivalents, in the form of malate, across the

mitochondrial membrane. The mitochondrial enzyme, in addition to its role in the other half of the malate shuttle, is also a necessary component of the tricarboxylic acid cycle.

Steady state studies of this enzyme, under conditions of ideal Michaelis-Menton behavior, have been interpreted in terms of a compulsory ordered mechanism (8, 9, 10) (see Appendix B) in which the coenzyme reactant is bound first, and the coenzyme product is released last in the rate-determining step. This mechanism is shown below in the notation of Cleland (11) (see Appendix B).



This interpretation has been supported by the work of Silverstein and Sulebele (12), using equilibrium isotope exchange methods. A reciprocating compulsory ordered mechanism (13, 14) earlier proposed as an amendment to the compulsory ordered mechanism has been discounted by these equilibrium exchange studies.

The Effects of Adenine Nucleotides

Studies of biochemical systems have suggested that adenine nucleotides may play an important role in the regulation of metabolic pathways. Specifically, the activity of malate dehydrogenase has been shown by several investigators to be affected by the presence of the nucleotide, ATP.

Williams (15) in 1951 first reported studies of the effect of ATP on rat liver homogenates containing malate dehydrogenase in 0.039 M equimolar Na-K phosphate buffer, pH 7.4 in the direction of NAD^+ reduction. For the observed competitive inhibition with respect to NAD^+ , he reported a $K_{i,\text{ATP}}$ of 16.4 mM and indicated that ATP inhibited twice as strongly as adenine.

Later studies by Angona, Ferrell, and Kitto (16) showed an inhibition of chicken heart and starfish, Pisaster borevispinus, malate dehydrogenases by AMP and cyclic 3',5'-AMP with respect to oxaloacetate. The reaction was likewise inhibited in the direction of NAD^+ reduction with inhibition competitive with respect to malate and noncompetitive with respect to NAD^+ .

Sanwal (17) with the E. coli enzyme in 0.15 M Tris-acetate buffer, 0.015 M EDTA, pH 7.4 and 9.0 found AMP, ADP, and ATP to inhibit enzymatic activity, but large concentrations were necessary to obtain significant inhibition. In the presence of 0.25 mM NAD^+ and 5.0 mM malate at pH 9.0, 4.5 mM ATP, 3.9 mM ADP, or 3.3 mM AMP was required to bring half-maximal inhibition. The high concentrations necessary for inhibition made it unlikely that these adenine nucleotides were involved intimately in the regulation of the E. coli enzyme in vivo. Further studies showed AMP to be a noncompetitive inhibitor with respect to NAD^+ . Nonlinear double reciprocal plots supported the conclusion that AMP caused inhibition at a site different from the NAD^+ binding site.

The most extensive studies of effects of adenine nucleotides have been done with the mitochondrial pig heart enzyme. Kuramitsu (18) in 1966 reported the effect of AMP, ADP, and ATP in both reaction

directions. In the direction of NADH oxidation in 0.033 M phosphate buffer, pH 7.4 at substrate levels of 0.047 mM NADH and 0.25 mM oxaloacetate, similar inhibitions were produced by all three nucleotides. With AMP the inhibition was of a mixed type with respect to oxaloacetate and competitive with respect to NADH. In 0.033 M Tris-Cl buffer, pH 8.8 at substrate levels of 1.0 mM NAD⁺ and 10.0 mM malate, all three adenine nucleotides acted as activators. The most potent activator, ATP, increased the enzymatic activity by a factor of two at ATP levels of 0.67-1.0 mM. For AMP an increased binding of NAD⁺ to the enzyme was observed, decreasing the apparent K_s for NAD⁺ with no alteration of V_{max} . The conclusion was that the enzyme had special allosteric sites for the adenine nucleotides.

Extension of his studies (19) to pea and other plant mitochondrial malate dehydrogenases in 0.10 M Tris-Cl buffer, pH 8.8 failed to show stimulation by any of the adenine nucleotides. ATP acted as a competitive inhibitor with respect to NAD⁺, increasing K_s for NAD⁺, and as a noncompetitive inhibitor with respect to malate lowering the K_s for malate. These findings suggested that the adenine nucleotides competed with NAD⁺ for the coenzyme site of the enzyme and did not act as allosteric inhibitors.

Finally, Oza and Shore (20) have also shown that ATP, ADP, and AMP act as competitive and uncompetitive inhibitors with respect to NADH and oxaloacetate, respectively. However, in 0.05 M Tris-acetate buffer, pH 8.0 only a 50-60% inhibition was observed at saturating concentrations of adenine nucleotides. Direct fluorescence titrations indicated that saturating concentrations of adenine nucleotides displaced only 50-60% of the bound NADH from the enzyme-NADH complex.

Despite these numerous studies, no investigators have utilized MgATP, the physiologically predominant form of ATP. In the present studies an extensive kinetic investigation of the effect of ATP and MgATP in the direction of NAD^+ reduction was undertaken to ascertain whether either nucleotide plays a significant role in metabolic regulation of porcine heart mitochondrial malate dehydrogenase. A 10 mM potassium phosphate buffer, 0.1 mM EDTA, pH 7.5 was selected as buffer system in view of the presence of phosphate in vivo near a cellular level of 10 mM and the specific ion effect of phosphate on the mitochondrial enzyme's activity. The catalytic optimum pH of 9.0 (10) was avoided due to its nonphysiological value.

Past investigators have overlooked the large ionic strength changes caused by ATP (changes up to 40 mM at 5 mM ATP). Relatively small variations in ionic strength as well as the qualitative composition of the ionic environment have been shown to affect the activity of mitochondrial malate dehydrogenase. The activating or inhibiting action of ions depends on the ion and its concentration, the substrate concentrations, the nature of the buffer, and the pH of the reaction medium.

For the mitochondrial enzyme from tea leaves in 0.5 M Tris-Cl buffer, pH 8.0, Tkemaladze et al. (21) have shown activation by NH_4Cl , KCl , CaCl_2 , MgCl_2 , and NaCl over the concentration range of 10^{-3} - 10^{-1} M. Further increases in ion concentration lead to inhibition. More pronounced effects of ions were observed in Tris-Cl buffer than in phosphate buffer.

For the ox kidney mitochondrial enzyme Dupourque and Kun (22) concluded that phosphate ion at pH 7.3 has two effects; it tends to

decrease oxaloacetate substrate inhibition and changes the apparent K_m for keto acid substrates. KCl behaves similarly; however, since the ionic strengths of the two ions differ, specificity of the ionic effect of phosphate as compared to chloride is not eliminated.

Kun, Eanes, and Volfin (7) have also shown an effect of phosphate on the oxaloacetate inhibition with rat kidney enzyme. As the level of phosphate is raised with constant ionic strength (KCl was used to maintain constant ionic strength), phosphate activates the enzyme. They suggested that the ionic environment was involved in regulation of mitochondrial metabolism.

Further ion studies by Weimberg (23) have shown that up to 30 mM NaCl has negligible effect on the activity of pea seed mitochondrial malate dehydrogenase in a 10.3 mM Tris-Cl buffer, pH 9.0 with 0.34 mM NAD^+ and 0.34 mM malate. At a level of 100 mM NaCl, the activity is reduced by half.

A report by E. J. Kresack (24) indicates that addition of magnesium ions to a Tris-acetate buffered system increased the activity of pig heart mitochondrial malate dehydrogenase. Similar effects by KCl suggested that stimulation was an ionic strength effect. Conversely, if phosphate buffer was substituted for Tris buffer, magnesium ions caused inhibition.

Blonde et al. (24) with pig heart mitochondrial malate dehydrogenase (in 100 mM Tris-acetate buffer, 0.76 mM oxaloacetate, 0.38 mM NADH, pH 7.4) have shown inhibition by $MgCl_2$, $MnCl_2$, $CaCl_2$, and KCl with slight stimulation at low ion concentrations (< 40 mM). Above approximately 10 mM, phosphate activated the enzyme; however, the presence of Mg^{2+} removed the stimulatory effect. These data indicate

that Mg^{2+} binds the phosphate involved in stimulation.

Finally, ion effect measurements have been performed in this laboratory (25) at low enzyme levels in the direction of NADH oxidation in 50 mM N-ethylmorpholine-HA buffer, pH 7.5 where A = F^- , Cl^- , Br^- , or NO_3^- . With mitochondrial porcine heart malate dehydrogenase numerous, large specific ion effects were demonstrated. For example, a negligible effect by KF below 250 mM was observed; however, 100 mM KCl and NaCl caused approximately a 24-27% inhibition which increased to 80% inhibition at 500 mM KCl. Tests with other ions showed that the degree of inhibition followed the sequence $KNO_3 > KBr > KCl > KF$ which was indicative of extensive specific anion effects.

In totality, these observations suggest that phosphate and ions in general play a very specific role in the structure of mitochondrial malate dehydrogenase. All previously reported investigations of ionic effects, except that by Weimberg (23) with tea leaf mitochondrial malate dehydrogenase, have been made in the direction of NADH oxidation in buffer systems differing from that used in the present studies. Thus an investigation of ionic effects in our buffer (10 mM potassium phosphate, 0.1 mM EDTA, pH 7.5) in the direction of NAD^+ reduction was necessary before studying the effects of ATP and MgATP. Also, since previous studies in our laboratory (25), as well as additional studies presented herein, suggested significantly altered and more stable behavior with concentrated enzyme ($\geq 10 \mu g/ml$), many of the following measurements were made with the stopped-flow fast kinetic method.

In summary, this study reports 1) effects of ionic strength and selected specific ions (K^+ , Na^+ , F^- , Cl^- , and Mg^{2+}) on mitochondrial porcine heart malate dehydrogenase in 10 mM potassium phosphate buffer,

0.1 mM EDTA, pH 7.5 in the direction of NAD^+ reduction, 2) effects of ATP and MgATP on the enzyme's kinetic properties in this buffer, and 3) identification of factors (enzyme concentration, buffer components, and pH) which alter the enzyme's kinetic constants and response to ATP. The latter study arose because the enzymatic properties in our system differed significantly from published results based principally on Tris buffer systems and dilute enzyme.

CHAPTER II

EXPERIMENTAL

Materials

NADH, ATP, NAD^+ , Trizma Base, ammonia color reagent (Nessler's Reagent), and Dowex-1 were from Sigma Chemical Company; EDTA and ultra-pure $(\text{NH}_4)_2\text{SO}_4$ from Schwarz-Mann; oxaloacetate (sodium salt) and malic acid from Calbiochem; and Amido Black 10B from K and K Laboratories, Inc. DL-tryptophan and DL-tyrosine were from Eastman Organic Chemicals and California Foundation for Biochemical Research, respectively. Porcine heart malate dehydrogenase was purchased from Sigma (Lot #54C95702, 1070 I.U./mg) and Miles Laboratories (Lot #R20A); alcohol dehydrogenase from Boehringer Mannheim GmbH; NaF and NaCl from Matheson Coleman and Bell; MgCl_2 from Mallinckrodt; $\text{Na}_4\text{P}_2\text{O}_7$, KCl, and KF from J. T. Baker Chemical Company; and KH_2PO_4 , K_3PO_4 , and Na_2HPO_4 from Fisher Scientific Company. DE32 diethylaminoethyl cellulose was from Whatman and Sephadex III cellulose acetate strips from Gelman Instrument Company.

Methods

Miscellaneous Reagent Preparations

All substrate solutions were freshly prepared on the day of use and the pH adjusted if necessary. MgCl_2 was further purified to remove

heavy metals by the method of Morrison and Uhr (26).

NAD^+ was initially further purified on the day of its use as described by Holbrook and Wolfe (27) to test for effects of the rapidly regenerated contaminant, which they have described. After washing with 250 ml of glass distilled water, NAD^+ was eluted from a 2 x 6 cm Dowex-1 column with 15 mM HCl. The pH and concentrations of phosphate and EDTA were adjusted to 7.5, 10 mM, and 0.1 mM, respectively. Since measured specific activities were not different from those obtained with commercial NAD^+ , this purification was eliminated from subsequent experiments. Diluted NAD^+ was allowed to remain as an acidic solution for one hour to destroy NADH impurities (28) prior to adjusting to pH 7.5. Final NAD^+ concentrations were determined 1) by absorbance at 260 nm assuming $\epsilon = 17.9 \text{ mM}^{-1}\text{cm}^{-1}$ or 2) by monitoring the production of NADH at 340 nm ($\epsilon = 6.22 \text{ mM}^{-1}\text{cm}^{-1}$) in an enzymatic assay with alcohol dehydrogenase. The final assay solution contained 0.1 M $\text{Na}_4\text{P}_2\text{O}_7$ buffer, pH 8.8, 0.34 M ethanol, 2.4×10^{-3} mg/ml alcohol dehydrogenase, and approximately 0.2 mM NAD^+ in 2.0 ml.

The concentration of ATP was determined by absorbance at 259 nm assuming $\epsilon = 15.4 \text{ mM}^{-1}\text{cm}^{-1}$. All initial velocity measurements were performed in 10 mM potassium phosphate buffer, 0.1 mM EDTA, pH 7.5 unless otherwise specified. At 10 mM phosphate and maximum Mg^{2+} concentrations used, no precipitates form.

Criteria of Enzyme Purity

The commercial Sigma enzyme was further purified with DE32 cellulose at 2-4°C. Prior to purification the enzyme was dialyzed against 1.67 mM potassium phosphate, 0.1 mM EDTA, pH 7.5 to remove $(\text{NH}_4)_2\text{SO}_4$.

Dialyzed enzyme (about 7 mg) was placed on a 2 x 8.5 cm column equilibrated with 0.1 M Tris-Cl buffer, pH 8.0 (28) or 1.67 mM potassium phosphate buffer, 0.1 mM EDTA, pH 7.5 at 2-4°C and eluted with the same buffer. Fluorescence spectra of purified peak fractions, unpurified enzyme, tyrosine, and tryptophan were recorded at an excitation of 275 nm (29).

Cellulose acetate electrophoresis of purified and unpurified enzyme was performed on 1.7 x 17 cm Sephapore III strips in 0.1 M Na_2HPO_4 buffer, pH 9.3 at 250 volts (25-27 amps) for three hours (29). A 1-40 μg protein sample was applied to each strip. Protein was stained by a modification of the method of Weiland and Dose (30). After electrophoresis the strips were dried to slight dampness with a hand-held dryer, fixed in 10% acetic acid in methanol, stained in a solution of 0.2 g Amido Black 10B in 1 liter of 10% aqueous acetic acid for one hour, and destained in 10% aqueous acetic acid.

Enzyme Preparation and Assay

Routine enzyme preparation consisted of centrifugation of the ammonium sulfate suspension at 17,500 rpm for 30 minutes, solution of the precipitated enzyme in buffer, and dialysis four times, each for 2-3 hours with 100 volumes of 10 mM potassium phosphate buffer, 0.1 mM EDTA, pH 7.5 in an argon atmosphere. The absence of $(\text{NH}_4)_2\text{SO}_4$ from the dialysate was ascertained with Nessler's Reagent. Routine enzyme preparation did not significantly alter the specific activity of the enzyme.

Changes in enzymatic activity during an experiment or from experiment to experiment were determined and correction factors applied

through the frequent use of a standard reference assay. Under most circumstances an experiment was entirely repeated if more than a 5% deterioration in enzyme activity occurred within a single day's experiment. Most dialyzed enzyme preparations were stable for at least a week. All specific activities were normalized by the ratio 657 I.U./mg \div (measured specific activity in standard reference assay). The standard reference assay contained 50 μ M oxaloacetate, 0.2 mM NADH, 10 mM potassium phosphate buffer, 0.1 mM EDTA, pH 7.5 in 2.0 ml in a 1 cm pathlength cuvette. The reaction at 340 nm was initiated by addition of appropriately diluted enzyme. Protein concentration was determined spectrophotometrically at 280 nm assuming $\epsilon = 0.28$ (mg/ml) $^{-1}$ cm $^{-1}$ (31). The gram molecular weight was assumed to be 70,000 g/mole. Specific activities based on the above assay were routinely 500-800 I.U./mg. Below 500 I.U./mg, a fresh preparation was made.

Instrumentation

Initial velocity measurements utilizing low enzyme concentrations, protein determinations, and NAD $^{+}$ and ATP concentration determinations were made in a Coleman 124 spectrophotometer equipped with a No. 0319 thermostatted cell holder, No. 801 scale expander, and a No. 165 recorder at 25°C in a 1 or 10 cm pathlength quartz cuvette (2 ml or 20 ml total solution, respectively). To measure small changes in absorbance, the full chart width was set for recording 0.1 absorbance unit.

Studies with concentrated enzyme were performed at 25°C in a Durrum-Gibson stopped-flow spectrophotometer with a tungsten light source. Absorbance changes at 340 nm in a 1.82 cm pathlength stopped-

flow cell were photographically recorded from a Tekronix storage oscilloscope. For stopped-flow measurements all buffers were deaerated for 10 minutes at room temperature in a water aspirator vacuum system. In all stopped-flow studies the disappearance of substrate was linear for a long enough period of time that determination of initial velocity was no problem.

Fluorescence spectra were obtained at 25°C in a thermostatted Aminco-Bowman spectrophotofluorometer with a xenon-mercury light source with 3 mm slit width in 1 cm pathlength quartz cuvettes. Monochromators were calibrated with a mercury pen-lamp and were within 3 nm of their correct values. Electrophoresis was carried out with a Gelman apparatus.

Data Analysis

The level of magnesium ion in a 10 mM potassium phosphate buffer necessary to give approximately 100% magnesium complexed ATP and 2 mM free Mg^{2+} at pH 7.5 was determined from dissociation constants calculated from data presented by Phillips et al. (32) for magnesium salts of ATP and Clark et al. (33) for magnesium salts of phosphoric acid. Ionic strength variations caused by varying levels of ATP were considered in calculations of the dissociation constants utilized in these computations. The desired 2 mM free Mg^{2+} was determined to be given by 3.2 mM excess of Mg^{2+} over total ATP concentration. The validity of calculations was verified by use of the computer routine COMICS (34) which computes equilibrium concentrations of species in mixtures of metal ions and complexing species.

Data obtained in ATP and MgATP inhibition studies which conformed

to a Bi Bi sequential initial velocity pattern (see Appendix B) with a single dead-end inhibitor (I) binding to the free enzyme form were fitted to Equation (2-1) where A and B represent NAD^+ and malate, respectively, v and V_{\max} are velocity and maximum velocity, respectively, and K_a and K_b represent the Michaelis constants for NAD^+ and malate, respectively. K_{ia} and K_i are the dissociation constants for NAD^+ and inhibitor (ATP and MgATP), respectively.

$$v = \frac{V_{\max} A B}{K_{ia} K_b \left(1 + \frac{I}{K_i}\right) + K_a B \left(1 + \frac{I}{K_i}\right) + K_b A + AB} \quad (2-1)$$

Least squares curve fitting of Equation (2-1) was done with the FORTRAN package MARQ (35) which finds a local minimum in the function F defined by Equation (2-2).

$$F = \sum_{i=1}^N \left\{ \frac{Y_{i,\text{exp}} - Y_{i,\text{calc}}}{\sigma_i} \right\}^2 \quad (2-2)$$

where $Y_{i,\text{exp}}$ is the measured velocity, $Y_{i,\text{calc}}$ is the computed velocity, and σ_i is the standard deviation in the measured velocity of the i th datum. The program prints out the fitted parameter values, errors in these values based on the usual linear approximation (36), the correlation among the parameters, and chi-square, an estimate of the quality of the fit (37) (the function F at the minimum equals chi-square).

CHAPTER III

RESULTS AND DISCUSSION

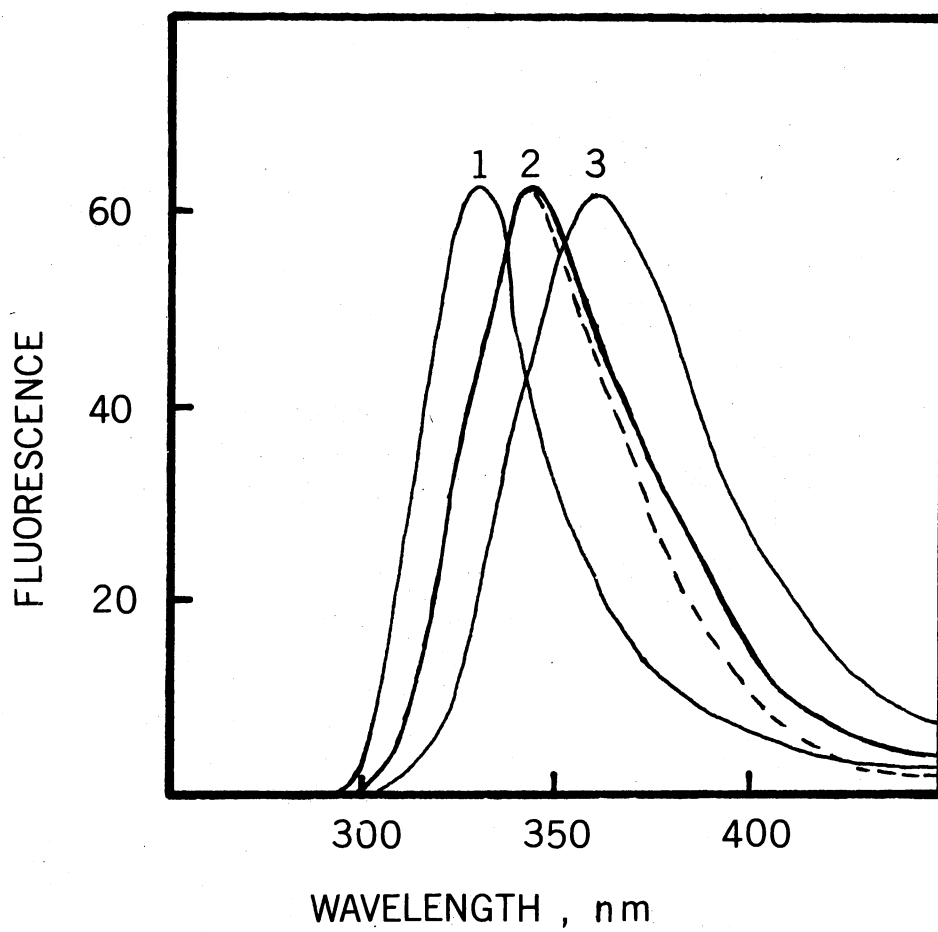
Criteria of Enzyme Purity

Purification of the commercial malate dehydrogenase resulted in only slightly improved specific activity regardless of which buffer system was used in column equilibration and elution. Chan and Schellenberg (29) also report negligible specific activity improvement by this chromatographic procedure.

Results of tests to ascertain the degree of purity of the Sigma preparation by the fluorometric criterion used by many investigators (20, 27, 29) were quite vague. Figure 1 shows spectra of tyrosine, tryptophan, purified peak enzyme fractions, and unpurified enzyme. The fluorometric criterion of purity is based on the fact that the mitochondrial enzyme contains no tryptophan ($\lambda_{\max} = 330 \text{ nm}$) (38) whereas the cytoplasmic enzyme does. When excited at 275 nm, the pure mitochondrial enzyme should have emission λ_{\max} at $307 \pm 5 \text{ nm}$, characteristic of the tyrosine residues.

Spectra obtained were distorted toward the red wavelength region. No specific cause of distortion could be ascertained. Despite the distortion, from comparison with the tyrosine and tryptophan spectra, the Sigma enzyme appeared to be quite pure. A small contaminant of tryptophan containing protein may be present which was removed by the

Figure 1. Fluorescence Spectra of Porcine Heart Mitochondrial Malate Dehydrogenase (Sigma - Lot #54C95702), Tyrosine, and Tryptophan. Spectra were obtained in 1.67 mM potassium phosphate buffer, 0.1 mM EDTA, pH 7.5. Excitation was at 275 nm. Spectra 1 and 3 are tyrosine and tryptophan, respectively. Spectrum 2 is a superposition of spectra obtained with unpurified enzyme (continuous line) and enzyme purified with a 1.67 mM potassium phosphate buffer, 0.1 mM EDTA, pH 7.5 equilibration-elution system (dashed line).



chromatography as evidenced by less tailing of the peak.

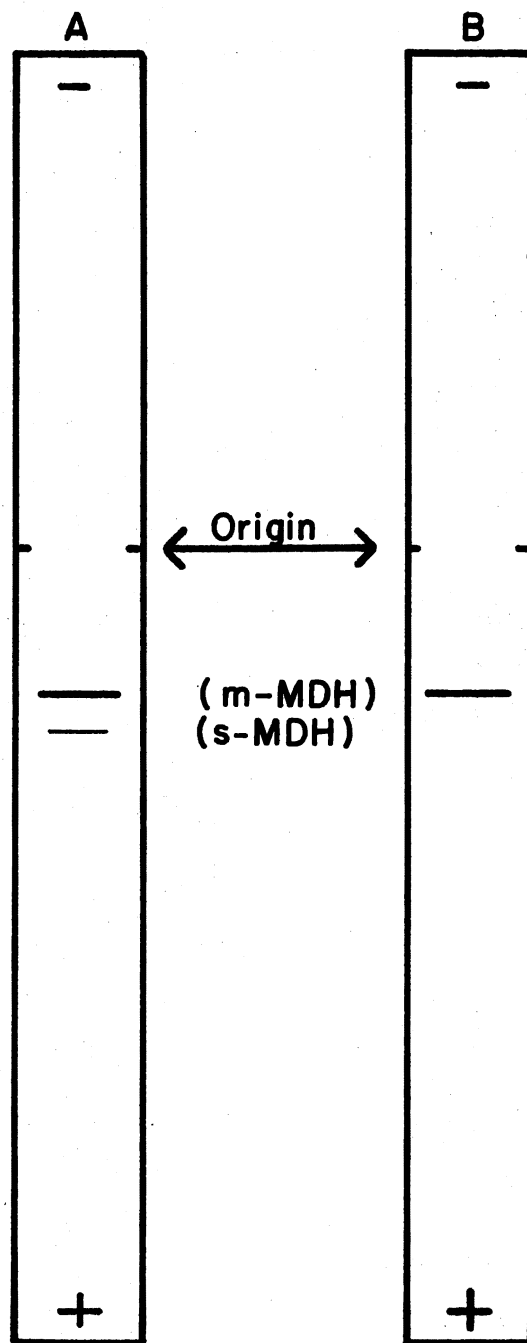
To substantiate this conclusion cellulose acetate electrophoresis was performed according to the method of Chan and Schellenberg (29) which separates the cytoplasmic and mitochondrial enzyme forms. Figure 2 shows typical electrophoresis results. The contaminating enzyme in the unpurified Sigma preparation was less than 5%. Despite which equilibration and elution buffer was used, purified enzyme showed only a single band verifying the removal of the cytoplasmic form. Since contamination of the commercial enzyme (Sigma-Lot #54C95702) was so small, it was used without further purification. Tests with another Sigma preparation (Lot #103C-9510) indicated that the quality of enzyme was variable. An enzyme preparation from Miles Laboratories (Lot #R20A) was also shown to contain 5% or less cytoplasmic contaminant.

Ionic Effects

The objectives of the following ionic effects studies were 1) to ascertain whether careful control of ionic strength was necessary in future ATP and MgATP measurements, 2) to test for a specific chloride ion effect, since Mg^{2+} was to be added to assay solutions as the $MgCl_2$ salt, and 3) to determine the effect on the enzyme's specific activity of 3.2 mM Mg^{2+} (approximate amount not to be complexed to ATP in later MgATP studies).

The effects of up to 100 mM KF, KCl, NaF, and NaCl on the activity of malate dehydrogenase were tested over a range of 0.08-1.0 mM NAD^+ with 1.0 mM malate. The salt concentration range of 0-100 mM was chosen, since a maximum level of 10 mM ATP (maximum concentration of ATP species in heart) was to be used in ATP and MgATP studies. Magnesium

Figure 2. Cellulose Acetate Electrophoresis of Pig Heart Malate Dehydrogenase. Strip A shows typical bands observed with 10 μ g unpurified Sigma enzyme (Lot #54C95702) where the upper and lower bands are mitochondrial and cytoplasmic enzymes, respectively. Strip B shows the single mitochondrial band observed with 10 μ g purified Sigma enzyme.



chloride at the level of 3.2 mM was tested over ranges of 1) 0.08-1.0 mM NAD⁺ at 1.0 mM malate and 2) 0.12-2.0 mM malate at 0.23 mM NAD⁺. All measurements were made in the stopped-flow spectrophotometer. The concentration of malate dehydrogenase was 7.5-10 µg/ml.

Table I summarizes the effects of KF, NaF, KCl, NaCl, and MgCl₂ on specific activities of mitochondrial malate dehydrogenase. KF and NaF over the range 0-100 mM had negligible effect on specific activities. KCl and NaCl significantly inhibited the enzyme activity above 35 mM, although inhibition was nonlinear in KCl concentration as shown in Figure 3 (nonlinear slope and intercept replots of double reciprocal plot). Little inhibition was observed below 35 mM KCl. Lack of effects by NaF and KF and identical effects by NaCl and KCl indicated that the enzyme was not affected by ionic strength increments of 100 mM in this buffer nor by Na⁺, K⁺, or F⁻, but was specifically inhibited by Cl⁻.

No effect of 3.2 mM MgCl₂ was observed over a wide range of substrate levels. Also at 5 mM ATP the maximum Cl⁻ concentration from addition of MgCl₂ is 16.4 mM (8.2 mM MgCl₂--approximately 5 mM to complex ATP, 2 mM free Mg²⁺, and 1.2 mM to complex HPO₄²⁻ as later shown) which is well below 35 mM where chloride ion inhibition appears. The use of MgF₂ in MgATP studies was prevented by its low solubility.

In summary, precautions to control ionic strength changes of up to 100 mM in this buffer system were unnecessary. Effects of 3.2 mM MgCl₂ and chloride ion below 35 mM were negligible.

ATP and MgATP Inhibition Studies

The objective of these studies was to determine whether ATP or

TABLE I
DEPENDENCE OF SPECIFIC ACTIVITY
ON PRESENCE OF IONS

[NAD ⁺] mM	[Salt] mM	Specific Activity ^a I.U./mg
1.0	No added salt	53.4 ^{b,d}
1.0	100 - KF	53.5
1.0	70 - KF	53.0
1.0	35 - KF	53.6
1.0	100 - NaF	53.6
1.0	100 - KCl	43.7 ^c
1.0	35 - KCl	51.7
1.0	15 - KCl	54.1
1.0	100 - NaCl	43.0
1.0	3.2 - MgCl ₂	53.5
0.16	No added salt	42.4
0.16	100 - KF	41.6
0.16	100 - KCl	30.1
0.16	3.2 - MgCl ₂	42.9
0.08	No added salt	34.4 ^b
0.08	100 - KF	33.2
0.08	70 - KF	34.4
0.08	35 - KF	34.6
0.08	100 - NaF	33.6
0.08	100 - KCl	22.8 ^c
0.08	35 - KCl	33.7

TABLE I (Continued)

0.08	15 - KCl	34.7
0.08	100 - NaCl	22.8
0.08	3.2 - MgCl ₂	34.7
0.23	No added salt	45.7
0.23	3.2 - MgCl ₂	46.1

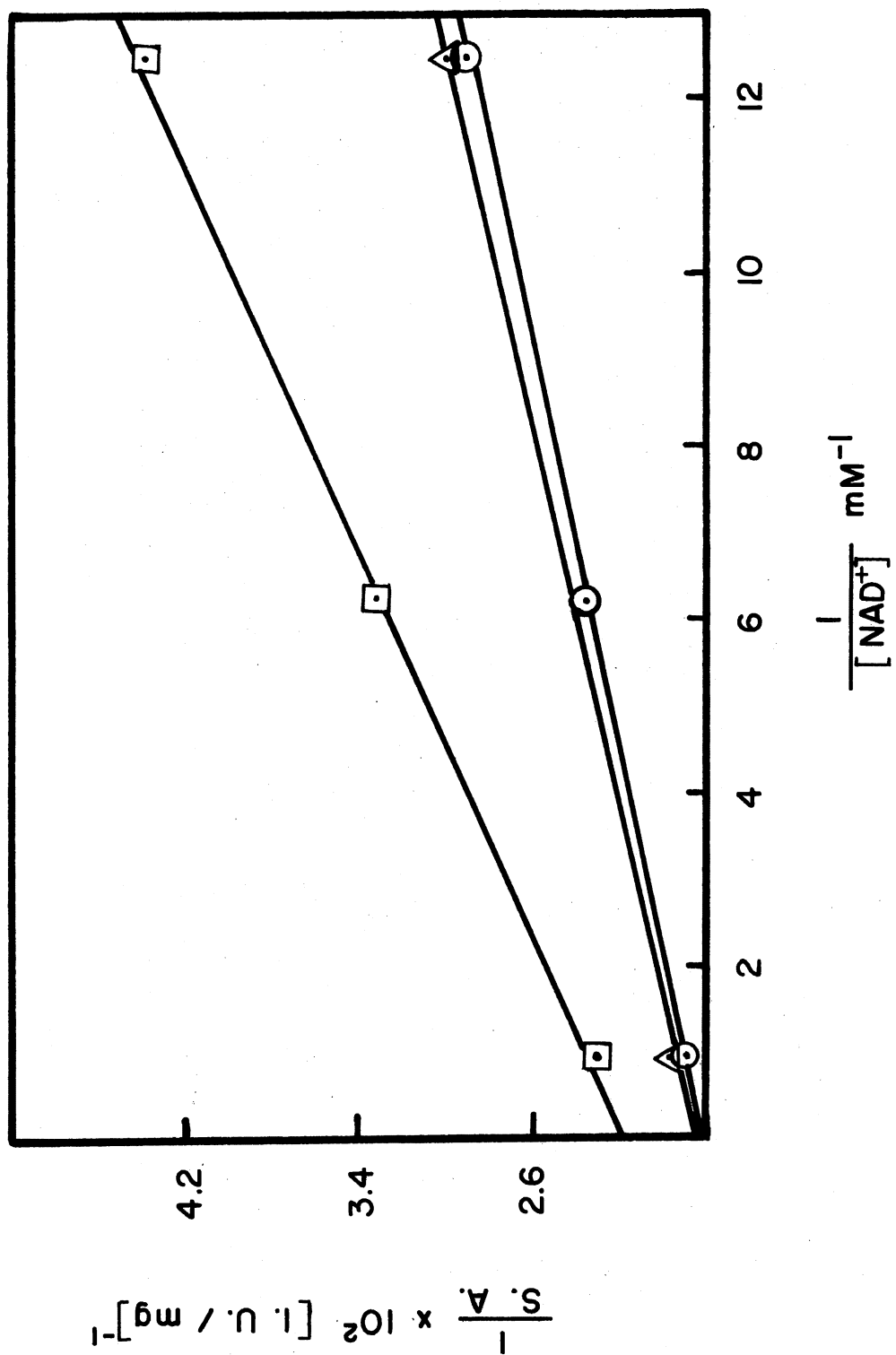
^aBuffer was 10 mM potassium phosphate, 0.1 mM EDTA, pH 7.5.
7.5-10 µg/ml malate dehydrogenase, 1.0 mM malate

^bThree separate multiple determinations

^cTwo separate multiple determinations

^dStandard deviations in specific activities were 0.3-1.9, based on at least three determinations.

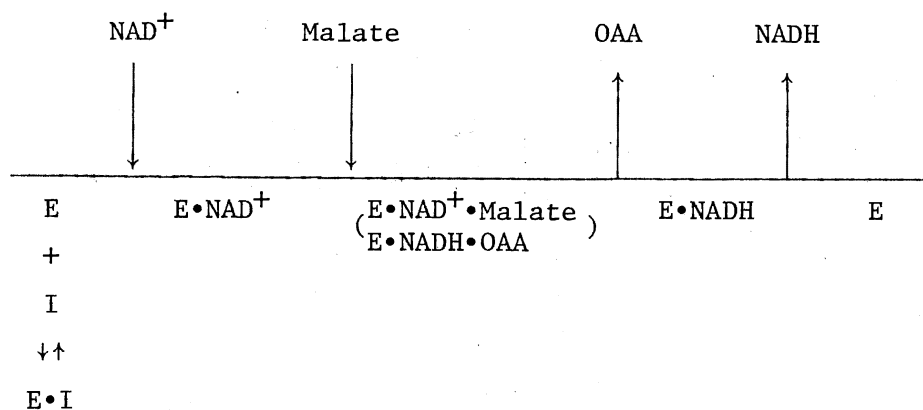
Figure 3. Inhibition of Porcine Heart Mitochondrial Malate Dehydrogenase by KCl. The malate concentration was fixed at 1.0 mM. Enzyme concentration was 10 μ g/ml. Buffer was 10 mM potassium phosphate, 0.1 mM EDTA, pH 7.5. KCl concentrations were 0.0 mM, \bigcirc — \bigcirc ; 35 mM, \triangle — \triangle ; and 100 mM, \square — \square .



MgATP at their physiological levels could act as metabolic regulators of mitochondrial malate dehydrogenase. Measurements were performed over the NAD^+ and malate ranges indicated in Figures 4-7 at enzyme levels of 7.5-60 $\mu\text{g}/\text{ml}$.

The levels of various Mg^{2+} complexed species and free ligands at three concentrations of ATP as computed in the COMICS routine are presented in Table II. A 3.2 mM excess of Mg^{2+} over total ATP concentration was used in calculations. As desired this level of excess Mg^{2+} gives approximately 2 mM free Mg^{2+} over a 0-10 mM ATP range.

The inhibitions caused by ATP and MgATP with respect to variation in NAD^+ and malate concentrations are shown in Figures 4-7. Fitted lines were obtained from fits to Equation (2-1). Both studies show competitive inhibition with respect to NAD^+ and noncompetitive inhibition with respect to malate with no apparent nonlinearity of inhibition in these concentration ranges. The most reasonable explanation for these inhibitions is binding of the inhibitor (I) to the free enzyme form as denoted below in the notation of Cleland (11) (see Appendix B).

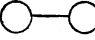
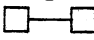
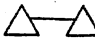
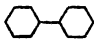


Two additional data points at low malate-high NAD^+ concentrations were necessary to obtain a value of K_b which was not highly correlated

TABLE II
 CONCENTRATIONS OF Mg²⁺ COMPLEXED SPECIES AND
 FREE LIGANDS IN PHOSPHATE BUFFER
 SYSTEM AS A FUNCTION OF
 ATP CONCENTRATION

Total [ATP] Containing Species ^a (mM)	[HPO ₄ ²⁻] (mM)	[H ₂ PO ₄ ⁻] (mM)	[MgHPO ₄] (mM)	[ATP ⁴⁻] (mM)	[HATP ³⁻] (mM)	[MgATP ²⁻] (mM)	[MgHATP ⁻] (mM)	[Mg ²⁺] (mM)
0	6.88	1.65	1.47	-----	-----	-----	-----	1.73
5	7.21	1.47	1.32	0.0535	0.0218	4.90	0.0257	1.96
10	7.47	1.33	1.20	0.117	0.0423	9.79	0.0502	2.16

^aCalculations performed at a level of 10 mM potassium phosphate at pH 7.5

Figure 4. Competitive Inhibition of Porcine Heart Mitochondrial Malate Dehydrogenase by ATP. Buffer was 10 mM potassium phosphate, 0.1 mM EDTA, pH 7.5. The malate concentration was fixed at 1.0 mM. Enzyme concentration was 10 μ g/ml. ATP concentrations were 0.0 mM, ; 0.75 mM, ; 1.5 mM, ; and 5.0 mM, .

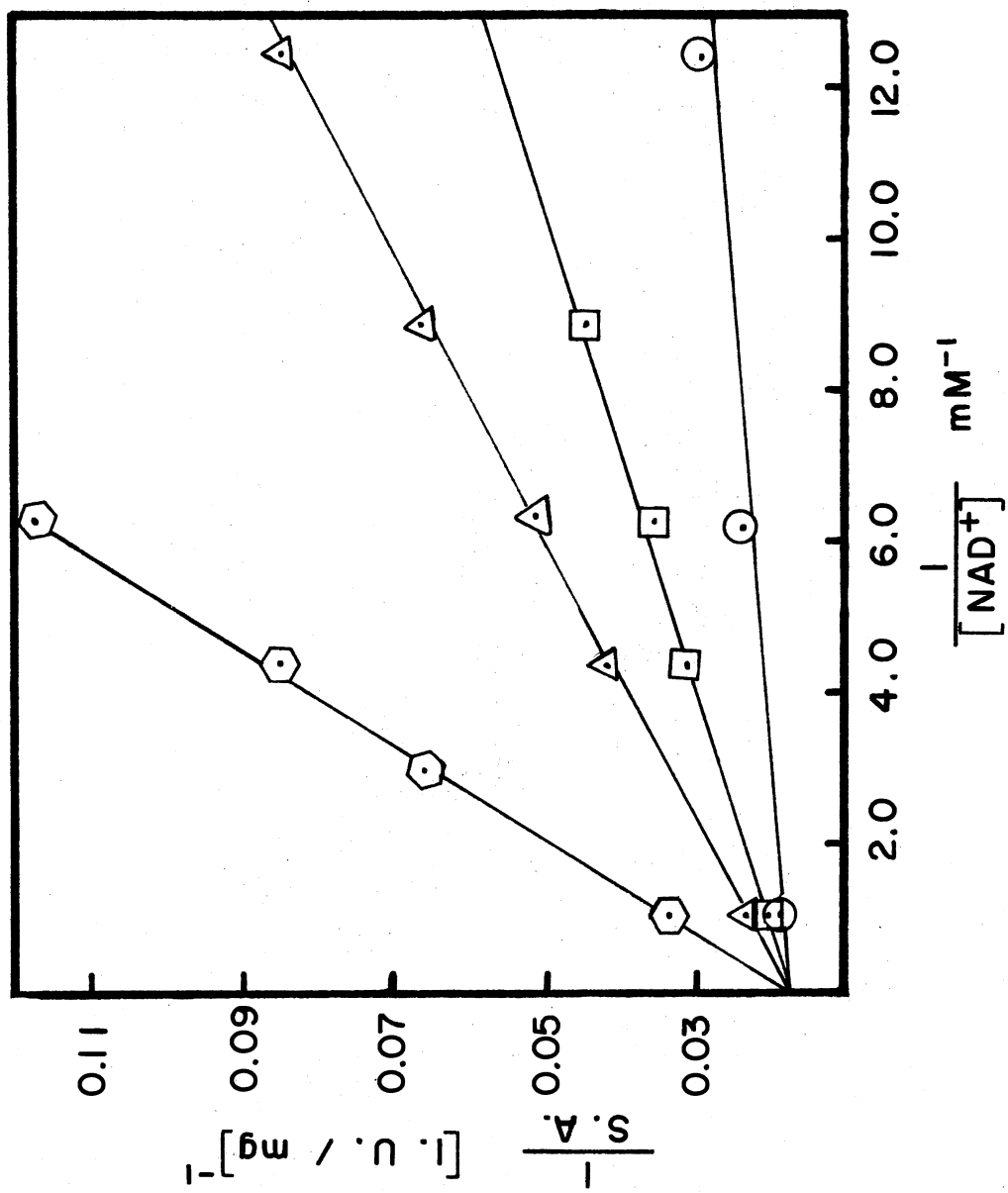
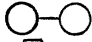
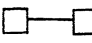
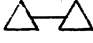
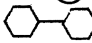


Figure 5. Noncompetitive Inhibition of Porcine Heart Mitochondrial Malate Dehydrogenase by ATP. Buffer was 10 mM potassium phosphate, 0.1 mM EDTA, pH 7.5. The NAD^+ concentration was fixed at 0.23 mM. Enzyme concentration was 10-60 $\mu\text{g}/\text{ml}$. ATP concentrations were 0.0 mM, ; 0.75 mM, ; 1.5 mM, ; and 3.0 mM, .

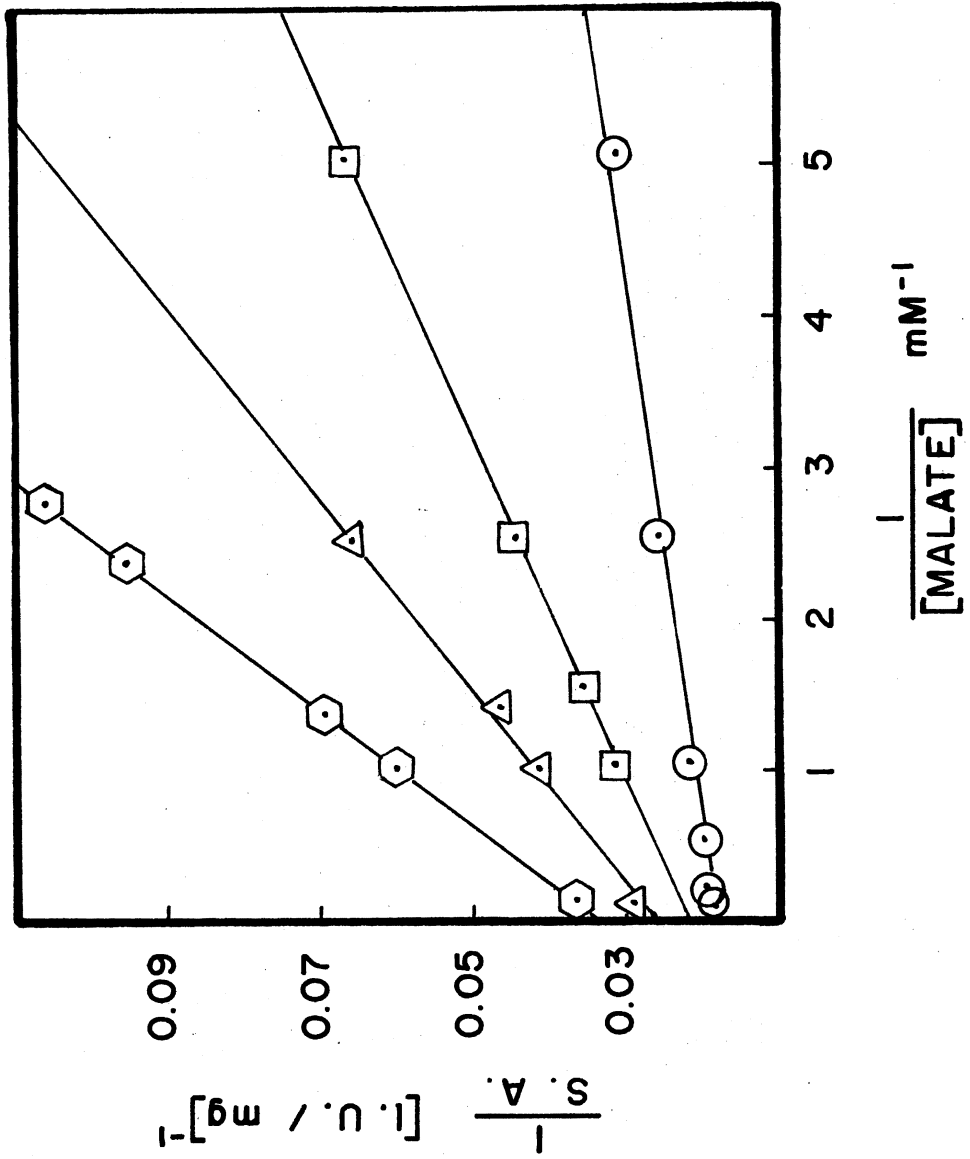
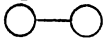
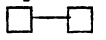
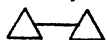
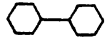


Figure 6. Competitive Inhibition of Porcine Heart Mitochondrial Malate Dehydrogenase by MgATP. Buffer was 10 mM potassium phosphate, 0.1 mM EDTA, pH 7.5. The malate concentration was fixed at 1.0 mM. Enzyme concentration was 10 μ g/ml. ATP and MgCl₂ concentrations were respectively: 0.0 mM and 3.2 mM, ; 1.5 mM and 4.7 mM, ; 3.0 mM and 6.2 mM, ; and 5.0 mM and 8.2 mM, .

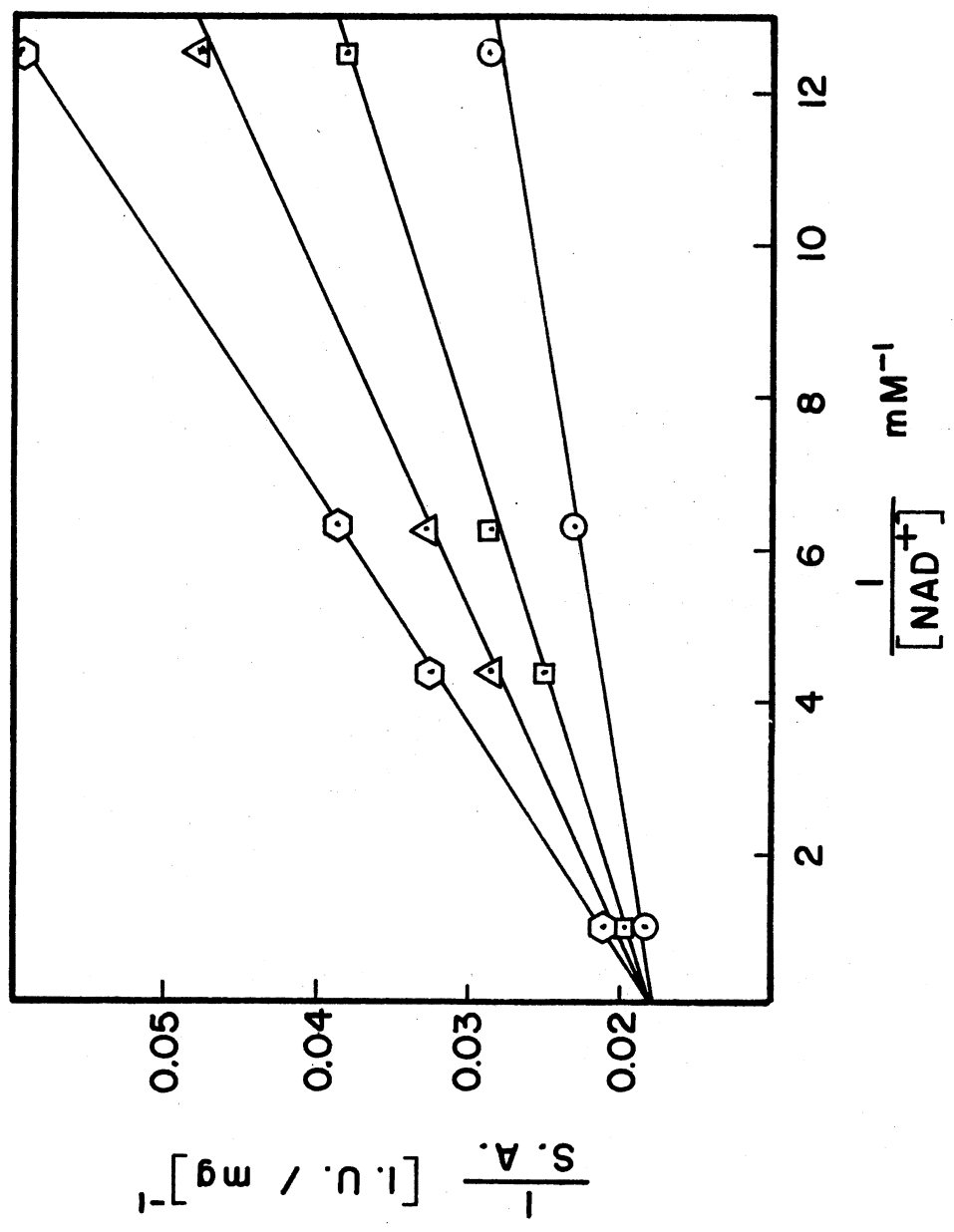
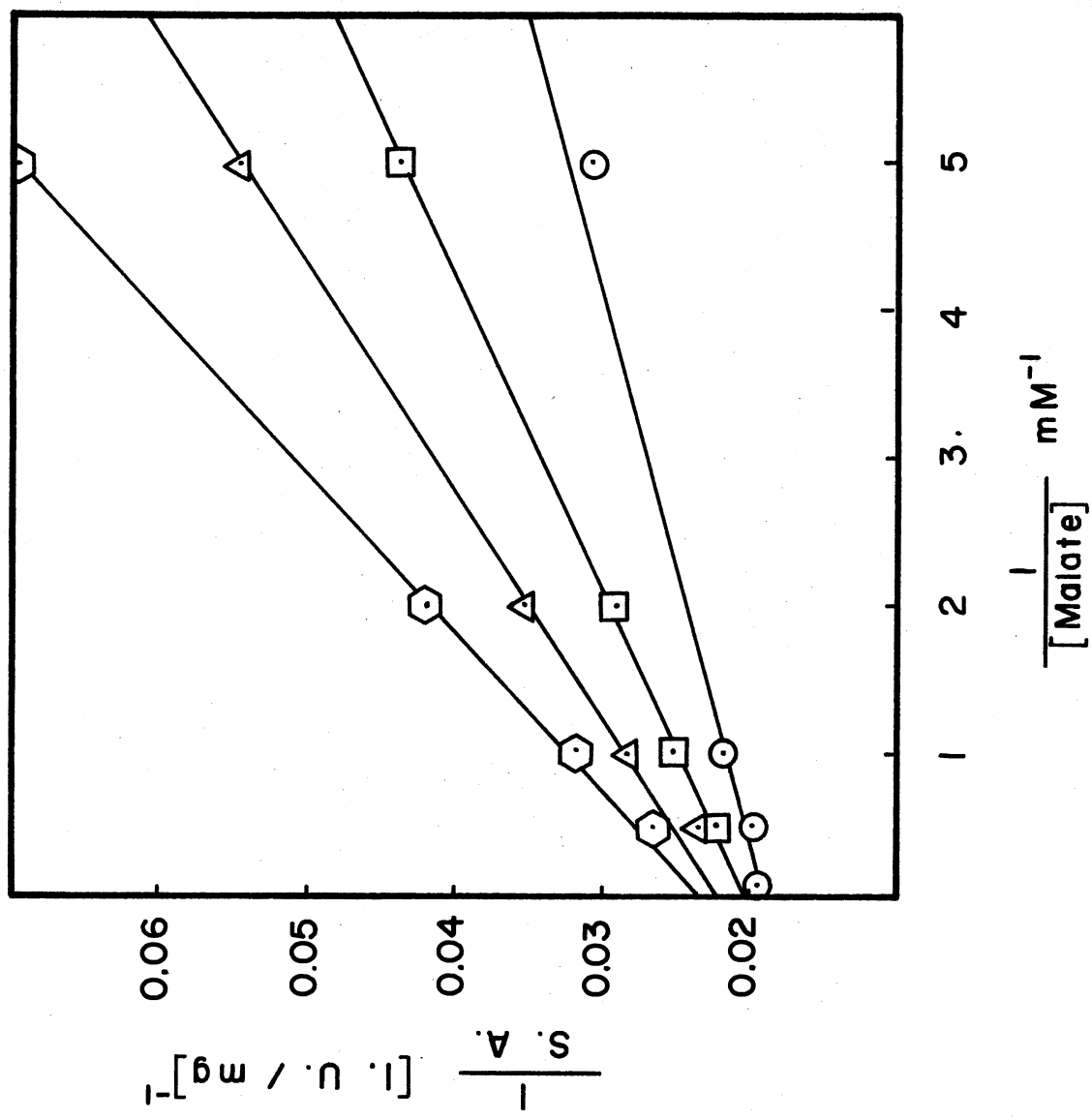


Figure 7. Noncompetitive Inhibition of Porcine Heart Mitochondrial Malate Dehydrogenase by MgATP. Buffer was 10 mM potassium phosphate, 0.1 mM EDTA, pH 7.5. The NAD^+ concentration was fixed at 0.23 mM. Enzyme concentration was 7.5 $\mu\text{g}/\text{ml}$. ATP and MgCl_2 concentrations were respectively: 0.0 mM and 3.2 mM, \bigcirc — \bigcirc ; 1.5 mM and 4.7 mM, \square — \square ; 3.0 mM and 6.2 mM, \triangle — \triangle ; and 5.0 mM and 8.2 mM, \hexagon — \hexagon .



with other parameters. Fitted parameters are given in Table III along with published literature values obtained in 0.05 M Tris-acetate buffer, pH 7.5 at 25°C (10). Good fits to Equation (2-1), characteristic of the established Bi Bi compulsory ordered mechanism, were obtained as attested to by the chi-square criterion of goodness-of-fit. A chi-square probability of 0.5 (maximum likely fit) was given by assuming 1.9% and 2.1% standard deviation in each velocity datum for the ATP and MgATP studies, respectively, a low yet reasonable estimated experimental error. Except for the K_i 's, the kinetic constants determined in ATP and MgATP inhibition studies are in excellent agreement. Agreement with literature values is poor. The most probable explanation for these deviations are 1) aberrant enzyme, 2) buffer system, and/or 3) enzyme concentration.

Not only do kinetic constants differ from published values but also ATP inhibition of enzyme is observed, contrary to the activation observed by Kuramitsu (18). The most notable experimental differences are again the buffer and enzyme concentrations utilized. It is interesting to note the agreement of these studies with those obtained with plant enzymes in 100 mM Tris-Cl buffer, pH 8.8 (19) and with the early studies of Williams (15).

With physiological NAD^+ , malate, and MgATP concentrations (39-43) estimated at 3 mM, 3 mM, and 10 mM (maximum reasonable level in heart) respectively, (observed velocity) $\div V_{\text{max}} = 0.93$. Thus it is unlikely that in vivo inhibition by MgATP functions to regulate the mitochondrial enzyme. Even though ATP is a more potent inhibitor, its much lower concentration than MgATP in vivo eliminates a significant physiological inhibition.

TABLE III
RESULTS OF REGRESSION ANALYSIS
OF INITIAL VELOCITY DATA

Parameter	ATP Inhibition Studies ^a	MgATP Inhibition Studies ^a	Literature Studies ^b
V_{\max}	58.3 I.U./mg $\pm 0.61^c$	57.7 I.U./mg ± 0.61	6000 M.A. (92.3 I.U./mg)
$10^2 \times K_a$	1.94 mM ± 0.12	1.90 mM ± 0.16	14 mM
$10^2 \times K_b$	3.48 mM ± 0.19	3.35 mM ± 0.21	80 mM
$10 \times K_{ia}$	8.23 mM ± 0.56	8.60 mM ± 0.72	7.5 mM
K_i	0.297 mM ± 0.011	1.66 mM ± 0.088	-----

^aBuffer was 10 mM potassium phosphate, 0.1 mM EDTA, pH 7.5. 7.5-60 μ g/ml enzyme

^bLiterature studies were done at low enzyme concentration in 0.05 M Tris-acetate buffer, pH 7.5. M.A. = moles of substrate decomposed per mole of enzyme per minute based on a molecular weight of 65,000 for the enzyme

^cError based on a linear approximation

Identification of Factors Altering Enzyme's Kinetic Properties

The objectives of these studies were 1) to explain the differences observed in the enzyme's kinetic constants in our phosphate buffer from earlier published values in 0.05 M Tris-acetate buffer, pH 7.5 and 2) to explain why inhibition rather than activation was observed in the present studies with ATP. The enzyme concentration and buffers used in measurements were investigated as most reasonable explanations.

Enzyme Concentration

Under a wide set of conditions, the specific activity of enzymes should be independent of enzyme concentration; however, under certain conditions, the catalytic behavior of enzymes is altered as they are concentrated.

Studies in Potassium Phosphate Buffer. These studies were conducted prior to measurements of ionic effects and ATP and MgATP effects and were the primary reason for using the stopped-flow method.

Studies by Spivey et al. (25) in the direction of NADH oxidation in phosphate buffer have suggested that at low enzyme levels (≤ 0.05 $\mu\text{g/ml}$) pig heart mitochondrial malate dehydrogenase is rapidly inactivated in the presence of low substrate concentrations. This conclusion has been primarily based on low and irreproducible activities at low substrate concentrations. Good reproducibility and higher activities were obtained at higher enzyme concentrations using stopped-flow methods.

To test for enzyme instability in the direction of NAD^+ reduction,

initial velocities were determined at enzyme concentrations of 50, 10, and 0.039 $\mu\text{g/ml}$ at high and low substrate concentrations: 1) 2.2 mM NAD^+ , 5.0 mM malate and 2) 0.16 mM NAD^+ , 0.30 mM malate. At low enzyme concentrations (Coleman spectrophotometer) malate dehydrogenase was used to initiate the reaction. At the higher enzyme levels (stopped-flow spectrophotometer) NAD^+ and enzyme were in one syringe and malate in the other. The specific activity ratios with high and low substrate concentrations, $\text{S.A.}_1/\text{S.A.}_2$, at each enzyme level were computed and compared.

These results are summarized in Table IV. Data at low substrate levels with 0.039 $\mu\text{g/ml}$ enzyme were extremely irreproducible (as much as 100% variation among repetitive initial velocity determinations) and disagreed substantially with specific activities at 10 and 50 $\mu\text{g/ml}$. Specific activities at higher substrate levels (2.2 mM NAD^+ , 5.0 mM malate) agreed within 5%, independent of enzyme concentration. The constant specific activities over the enzyme range of 10-50 $\mu\text{g/ml}$ indicates that at high protein levels the enzyme concentration is not affecting kinetic behavior. The difference in specific activities at low enzyme-low substrate levels suggests 1) the enzyme's kinetic behavior depends on protein concentration and/or 2) the enzyme is being inactivated at low enzyme-low substrate levels. A conclusion of inactivation is supported by the irreproducibility and the measurement of essentially zero activity when a low concentration of enzyme is incubated with 0.16 mM NAD^+ for longer than 1 minute in the reaction cuvette before starting the reaction. Whether the low specific activity is caused entirely by enzyme instability or is a superimposition of instability and differing catalytic properties at low and high enzyme concentrations is

TABLE IV
 DEPENDENCE OF SPECIFIC ACTIVITY ON ENZYME
 CONCENTRATION AT HIGH AND LOW
 SUBSTRATE LEVELS

[MDH] ^c μg/ml	Specific Activity ^{a,b} I.U./mg		S.A. ₁ /S.A. ₂
	Condition 1	Condition 2	
10	55.8 ± 0.7 ^d	33.5 ± 0.7	1.7
20	56.5 ± 1.3	33.8 ± 0.4	1.7
0.039	53.9 ± 3.1	12.6 ± 4.5	4.3

^aCondition 1 consists of 2.2 mM NAD⁺, 5.0 mM malate.

^bCondition 2 consists of 0.16 mM NAD⁺, 0.30 mM malate.

^cBuffer was 10 mM potassium phosphate, 0.1 mM EDTA, pH 7.5.

^dStandard deviation based on at least triplicate determinations

yet unclear. No investigators have suggested enzyme inactivation at low substrate levels in other buffer systems. Although J. D. Shore (44) reports dissociation of the enzyme dimer to monomers at low enzyme concentrations ($K_d = 2 \times 10^{-7} \text{ N}$), monomer and dimer have identical specific activities in both reaction directions in Tris buffer. Thus enzyme dissociation does not explain low, irreproducible specific activities at low enzyme concentrations unless potassium phosphate buffer affects the relative activities of monomer-dimer in a different manner than Tris buffer. Frieden and Fernandez-Sousa (45) have reported instability below 5-10 $\mu\text{g/ml}$ with pig heart cytoplasmic malate dehydrogenase in sodium phosphate buffer.

Similar inhibitions with 1.0 mM ATP were observed at both low (0.031-0.038 $\mu\text{g/ml}$) and high (10-60 $\mu\text{g/ml}$) enzyme concentrations in potassium phosphate buffer in the presence of 0.23-1.0 mM NAD^+ and 1.0-10 mM malate.

In summary, the effect of enzyme concentration on kinetic behavior (and thus the kinetic constants) in 10 mM potassium phosphate buffer, 0.1 mM EDTA, pH 7.5 is yet questionable due to the difficulty in obtaining reproducible initial velocities at the low substrate concentrations necessary to obtain these constants. Measurements suggest that the kinetic behavior is not a function of enzyme concentration at and above 7.5 $\mu\text{g/ml}$. Also the ATP effect is independent of enzyme concentration.

Studies in Tris Buffers. The effect of varying enzyme concentration on 1) the ATP effect observed by Kuramitsu (18) in 0.033 M Tris-Cl buffer, pH 8.8 and 2) the kinetic constants reported by Raval and Wolfe

(10) in 0.05 mM Tris-acetate buffer, pH 7.5 were examined in these buffers.

The dependence of the ATP effect on enzyme concentration over the range of 0.023-20 $\mu\text{g/ml}$ was determined in 0.033 M Tris-Cl buffer, pH 8.8 in the presence of 1.0 mM NAD^+ and 10 mM malate (same assay conditions as used by Kuramitsu except at both high and low enzyme concentrations). Kuramitsu's observation of a two-fold activation by 1.0 mM ATP at low enzyme concentrations was confirmed. Specific activities over an enzyme range of 0.023-20 $\mu\text{g/ml}$ as well as the degree of activation by 1.0 mM ATP (two-fold increase in activity) were also in good agreement. Together with results in the potassium phosphate buffer, these observations eliminate an enzyme concentration dependence of the ATP effect in both buffers.

A thorough laborious steady state analysis at both low and high enzyme levels in 0.05 M Tris-acetate buffer, pH 7.5 would definitively establish whether high enzyme concentration affects the values of reported kinetic constants determined at low enzyme concentrations by Raval and Wolfe (10). Alternatively, since the values of the kinetic constants determined in our potassium phosphate buffer system differ by at least a factor of 10, approximate constants could be obtained in the Tris-acetate buffer at high enzyme concentration by fixing one substrate at a saturating level and lowering the other substrate concentration to approximately its K_m value. However, published accounts reveal that at the high levels necessary to saturate with these substrates, NAD^+ and malate, respectively, inhibit and activate the enzyme in the Tris-acetate buffer system (8). This makes a simplified approach to the kinetic constants unrealistic.

As a third alternative, specific activities were determined under two sets of substrate conditions: 1) 1.0 mM NAD^+ , 0.8 mM malate and 2) 0.14 mM NAD^+ , 1.0 mM malate in 0.05 M Tris-acetate buffer, pH 7.5 at 10 $\mu\text{g/ml}$ and 9.02×10^{-3} $\mu\text{g/ml}$ enzyme levels. The ratio of these specific activities were compared with the theoretical ratio (2.45) calculated from published constants in 0.05 M Tris-acetate buffer, pH 7.5 and the theoretical ratio (1.26) calculated from constants at high enzyme levels determined in 10 mM potassium phosphate buffer, 0.1 mM EDTA, pH 7.5. The measured ratios in the Tris-acetate buffer system at 10 $\mu\text{g/ml}$ and 9.02×10^{-3} $\mu\text{g/ml}$ were 2.28 and 2.31, respectively, which are both in good agreement with the ratio calculated from literature values. Specific activities at the two enzyme concentrations for each substrate condition agreed within 8%. These results indicate that the kinetic constants in the Tris-acetate system are unaffected by a higher enzyme concentration. While this method does not yield numerical values of the kinetic constants, if the constants differed substantially at high enzyme concentration in the Tris-acetate buffer system, this difference should have been reflected in the specific activity ratio obtained. The kinetic constants obtained in the potassium phosphate buffer system are not applicable to the enzyme in 0.05 M Tris-acetate, pH 7.5 regardless of enzyme concentration.

In summary, enzyme concentration does not explain the difference observed in the kinetic constants of mitochondrial porcine heart malate dehydrogenase or its behavior toward ATP. Thus the most reasonable explanation is a buffer influence on the catalytic properties of the enzyme.

Buffer Components

Initial velocities in the presence and absence of 1.0 mM ATP at 1.0 mM NAD^+ , 10 mM malate, and low enzyme concentrations (0.023-0.055 $\mu\text{g/ml}$) were determined in several buffer systems in order to test for effects of pH, K^+ , Cl^- , Tris^+ , phosphate, and EDTA on enzyme behavior toward ATP. Table V summarizes results of these studies. The buffer systems and their corresponding variables were 1) pH - buffers 1-4, 2) Cl^- - buffers 8-10, 3) K^+ - buffers 6 and 7, 4) EDTA - buffer 5, and 5) Tris^+ and phosphate - buffers 11 and 12. Slight differences in enzymatic activity were observed in 0.033 M Tris-Cl buffer, pH 8.8 depending on whether the reaction was initiated with enzyme or malate. The magnitude of ATP effect, however, was not altered by the nature of the initiator. Reported results were obtained with malate as the initiator, since all stopped-flow measurements utilized malate as initiator. In 10 mM potassium phosphate buffer, 0.1 mM EDTA, pH 7.5 no dependence on initiator was observed.

Although pH change from 8.8 to 7.5 lowered the degree of activation in Tris-Cl buffer, the overall effect was yet activation. Addition of EDTA to the Tris-Cl buffer also failed to change the degree of activation. Nor did Cl^- added to the potassium phosphate buffer at the levels present in 0.033 M Tris-Cl, pH 7.5 and 8.8 change the degree of ATP inhibition in potassium phosphate buffer. Addition of K^+ at the level in potassium phosphate buffer in the Tris-Cl buffer also produced a negligible change in the degree of activation. However, addition of Tris-Cl or Tris-F at the level in 0.033 M Tris-Cl, pH 7.5 to the potassium phosphate buffer not only reversed the inhibition exhibited

TABLE V
EFFECTS OF BUFFER SYSTEM COMPONENTS
ON ENZYME BEHAVIOR IN THE
PRESENCE OF ATP

Buffer Number	Buffer Composition ^a	% Activity
1	10 mM potassium phosphate, 0.1 mM EDTA, pH 7.5	92 ± 6 ^c
2	0.033 M Tris-Cl, pH 7.5	169 ± 6
3	0.033 M Tris-Cl, pH 8.8	196 ± 4
4	10 mM potassium phosphate, 0.1 mM EDTA, pH 8.8	92 ± 2
5	0.033 M Tris-Cl, 0.1 mM EDTA, pH 8.8	196 ± 7
6	0.033 M Tris-Cl, 17.56 mM KF, pH 8.8	192 ± 6
7	0.033 M Tris-Cl, 17.56 mM KCl, pH 8.8	192 ± 5
8	10 mM potassium phosphate, 0.1 mM EDTA, 9.40 mM KCl, pH 7.5	92 ± 8
9	10 mM potassium phosphate, 0.1 mM EDTA, 29.31 mM KCl, pH 7.5	92 ± 8
10	10 mM potassium phosphate, 0.1 mM EDTA, 9.40 mM KCl, pH 8.8	91 ± 3
11	10 mM potassium phosphate, 0.1 mM EDTA, 0.033 M Tris-F, pH 7.5	171 ± 7
12	10 mM potassium phosphate, 0.1 mM EDTA, 0.033 M Tris-Cl, pH 7.5	171 ± 5

^a0.034-0.055 µg/ml enzyme, 1 mM NAD⁺, 10 mM malate

^b(Specific activity with 1 mM ATP/Specific activity without ATP) X 100

^cFractional standard deviation based on at least 3 determinations

in potassium phosphate buffer to the activation observed in 0.033 M Tris-Cl, pH 7.5 but also changed the specific activity measured in potassium phosphate buffer (buffer 1) to the value measured in Tris-Cl (buffer 2). From these results the most likely components affecting the enzyme's behavior toward ATP are Tris^+ and phosphate; however, in the presence of both at the specified concentrations, Tris^+ dictates the effect. These results are not completely definitive; however, it is apparent that the ATP effect depends on the buffer system.

Whether inhibition or activation is the physiological reality is questionable; however, due to the physiological presence of phosphate it is difficult to discount its importance relative to Tris^+ . That potassium phosphate and Tris-Cl buffer systems cause behavioral differences in mitochondrial malate dehydrogenase has been previously suggested. Joyce and Grisolia (46) state that in potassium phosphate buffer relative to Tris-Cl under identical assay conditions the enzyme is four times as active in phosphate buffer. In studies of Hg(II) effects on mitochondrial malate dehydrogenase from pig heart, Kuramitsu (47) suggests that the structure of the enzyme may differ in potassium and Tris-Cl buffers at the same pH due to his observation that Hg(II) produces opposing effects in Tris-Cl (activation) and phosphate (inhibition) buffers. Binding of phosphate and chloride anions to the enzyme or a buffer induced conformational change was suggested as a possible explanation for these structural differences. These indications of buffer regulated behavior of the mitochondrial pig heart enzyme together with the ionic effects related in the Introduction suggest that results of investigations with porcine heart mitochondrial malate dehydrogenase

may be highly dependent upon the environment in which the enzyme is studied.

CHAPTER IV

SUMMARY AND CONCLUSION

These studies have shown ATP and MgATP to inhibit mitochondrial porcine heart malate dehydrogenase with $K_{i,ATP} = 0.28$ mM and $K_{i,MgATP} = 1.7$ mM in 10 mM potassium phosphate buffer, 0.1 mM EDTA, pH 7.5. Since at estimated physiological levels of ATP, MgATP, malate, and NAD^+ , insignificant inhibition is observed, ATP and MgATP probably do not serve to regulate the behavior of the enzyme.

Of major importance, these studies suggest that the catalytic properties of the enzyme are highly dependent upon the environment in which the enzyme is studied, and precautions should be observed in stating definitive behavior of the enzyme in vivo. This indication stresses the extreme importance of designing systems of enzyme study based on consideration of cellular conditions. As a guiding factor we have attempted to conduct enzyme studies in an environment which was as near to physiological conditions as our experimental objectives allowed.

A SELECTED BIBLIOGRAPHY

- (1) Banaszak, L. J. and Bradshaw, R. A. (1975) in *The Enzymes*, P. D. Boyer, ed., Vol. XI, pp. 369-396. Academic Press, New York.
- (2) Kitto, G. B. and Kaplan, N. O. (1966) *Biochemistry*, 5, 3966-3980.
- (3) Kitto, G. B. and Wilson, A. C. (1966) *Science*, 153, 1408-1410.
- (4) Devenyi, T., Rogers, S. J., and Wolfe, R. G. (1966) *Nature*, 210, 489-491.
- (5) Kun, E. and Volfin, P. (1966) *Biochem. Biophys. Res. Comm.*, 22, 187-193.
- (6) Thorne, C. J. R. and Kaplan, N. O. (1963) *J. Biol. Chem.*, 238, 1861-1868.
- (7) Kun, E., Eanes, R. Z., and Volfin, P. (1967) *Nature*, 214, 1328-1330.
- (8) Raval, D. N. and Wolfe, R. G. (1962) *Biochemistry*, 1, 263-269.
- (9) Raval, D. N. and Wolfe, R. G. (1962) *Biochemistry*, 1, 1112-1117.
- (10) Raval, D. N. and Wolfe, R. G. (1962) *Biochemistry*, 1, 1118-1123.
- (11) Cleland, W. W. (1963) *Biochim. Biophys. Acta*, 67, 104-137.
- (12) Silverstein, E. and Sulebele, G. (1969) *Biochemistry*, 8, 2543-2550.
- (13) Harada, K. and Wolfe, R. G. (1968) *J. Biol. Chem.*, 243, 4123-4130.
- (14) Harada, K. and Wolfe, R. G. (1968) *J. Biol. Chem.*, 243, 4131-4137.
- (15) Williams, J. N. (1952) *J. Biol. Chem.*, 195, 629-635.
- (16) Angona, R. G., Ferrell, R., and Kitto, G. B. (1968) *Abstracts South Western Regional A. C. S. Meeting, Tulsa, Oklahoma, No. 48.*

- (17) Sanwal, B. D. (1969) *J. Biol. Chem.*, 244, 1831-1837.
- (18) Kuramitsu, H. K. (1966) *Biochem. Biophys. Res. Comm.*, 23, 329-334.
- (19) Kuramitsu, H. K. (1968) *Arch. Biochem. Biophys.*, 125, 383-384.
- (20) Oza, N. B. and Shore, J. D. (1973) *Arch. Biochem. Biophys.*, 154, 360-365.
- (21) Tkemaladze, G. Sh., Morchiladze, Z. N., Soseliya, M. F., and Kretovich, V. L. (1972) *Biokhimiia*, 37, 1003-1006.
- (22) Dupourque, D. and Kun, E. (1969) *Eur. J. Biochem.*, 7, 247-252.
- (23) Weimberg, R. (1967) *J. Biol. Chem.*, 242, 3000-3006.
- (24) Blonde, D. J., Kresack, E. J., and Kosicki, G. W. (1967) *Can. J. Biochem.*, 45, 641-650.
- (25) Spivey, H. O., Blanton, L. S., McCaslin, D. R., and Taylor, D. J., personal communication.
- (26) Morrison, J. F. and Uhr, M. L. (1966) *Biochim. Biophys. Acta*, 122, 57-74.
- (27) Holbrook, J. J. and Wolfe, R. G. (1972) *Biochemistry*, 11, 2499-2502.
- (28) Lowry, O. H., Passonneau, J. V., and Rock, M. K. (1961) *J. Biol. Chem.*, 236, 2756-2759.
- (29) Chan, T-L and Schellenberg, K. A. (1968) *J. Biol. Chem.*, 243, 6284-6290.
- (30) Wieland, T. and Dose, K. (1954) *Biochemische Zeitschrift*, 325, 439-447.
- (31) Thorne, C. J. R. (1962) *Biochim. Biophys. Acta*, 59, 624-633.
- (32) Phillips, R. C., George, P., and Rutman, R. J. (1966) *J. Amer. Chem. Soc.*, 88, 2631-2640.
- (33) Clarke, H. B., Cusworth, D. C., and Datta, S. P. (1954) *Biochem. J.*, 58, 146-154.
- (34) Perrin, D. D. and Sayce, I. G. (1967) *Talanta*, 14, 833-842.
- (35) Marquardt, D. W. (1963) *J. S. I. A. M.*, 11, 431-441.
- (36) Bevington, P. R. (1969) *Data Reduction and Error Analysis for the Physical Sciences*, McGraw-Hill Book Company, New York.

- (37) Hamilton, W. C. (1969) *Statistics in the Physical Sciences*, Ronald Press Company, New York.
- (38) Eberhardt, N. L. and Wolfe, R. G. (1974) *Arch. Biochem. Biophys.*, 160, 151-155.
- (39) Büchner, T. (1970) in *Pyridine Nucleotide-dependent Dehydrogenases*, H. Sund, ed., pp. 439-461. Springer-Verlag, New York.
- (40) Williamson, J. R. (1969) in *the Energy Level and Metabolic Control in Mitochondria*, S. Papa, E. Quagliariello, and E. C. Slater, eds., pp. 385-400. Adriatica Editrice, Bari.
- (41) Krebs, H. A. and Veech, R. L. (1970) in *Pyridine Nucleotide-dependent Dehydrogenases*, H. Sund, ed., pp. 413-438. Springer-Verlag, New York.
- (42) Greenbaum, A. L., Guma, K. A., and McLean, P. (1971) *Arch. Biochem. Biophys.*, 143, 617-663.
- (43) Humle, E. C. and Tipton, K. F. (1971) *FEBS Lett.*, 12, 197-200.
- (44) Shore, J. D. and Weidig, C. F. (1975) *Fed. Proc.*, 34, Abstract 1974.
- (45) Frieden, C. and Fernandez-Sousa, J. (1975) *J. Biol. Chem.*, 250, 2106-2111.
- (46) Joyce, B. K. and Grisolia, S. (1961) *J. Biol. Chem.*, 236, 725-729.
- (47) Kuramitsu, H. K. (1968) *J. Biol. Chem.*, 243, 1016-1021.

PART TWO

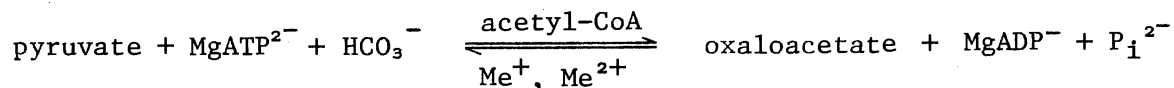
LIGAND INDUCED CONFORMATIONAL TRANSITIONS
AND SECONDARY STRUCTURE COMPONENTS OF
CHICKEN LIVER PYRUVATE
CARBOXYLASE

CHAPTER I

INTRODUCTION

Selected Properties of Pyruvate Carboxylase

Pyruvate carboxylase (1, 2, 3) (pyruvate: CO₂ ligase (ADP); EC 6.4.1.1.) catalyzes the following reaction.



Me⁺ and Me²⁺ are univalent and divalent cations, respectively.

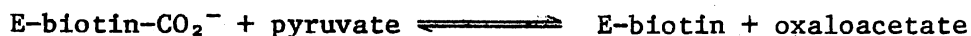
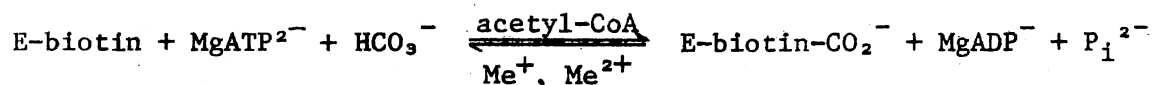
The enzyme is found in bacteria, yeast, mold, fungi, insects, aves, and mammals; however, the kinetic and physical properties differ considerably from species to species. In aves and mammals the enzyme is present at high levels in liver, kidney, and adipose tissue and at lower but significant levels in brain and mammary tissue. The extensive tissue and species distribution of pyruvate carboxylase reflects the multiple roles proposed for the enzyme in metabolism. These include involvement in 1) gluconeogenesis, 2) anaplerotic synthesis of oxaloacetate, and 3) NADPH supply for fatty acid synthesis in adipose tissue.

All species of pyruvate carboxylase tested thus far require the presence of a divalent cation as Mg²⁺ and monovalent cation as K⁺ for activity; however, there is a widespread difference in the requirement for an acyl-CoA activator. Since for the chicken liver enzyme the requirement is essentially absolute, this allosteric activator has been

proposed as a possible regulator of the enzyme.

Pyruvate carboxylase from the liver of chicken is composed of four subunits arranged at the corners of a square. The enzyme contains four biotinyl groups and four tightly bound manganese or magnesium ions. In the presence of acetyl-CoA, it is highly susceptible to inactivation at low temperatures and dissociates to almost inactive monomers.

A minimal reaction mechanism for pyruvate carboxylase has been proposed on the basis of isotope exchange studies and the isolation of an enzyme-biotin-CO₂ complex.



In summary, the major features of the reaction mechanism for chicken liver pyruvate carboxylase are the following: 1) the overall reaction is the sum of two partial reactions and can be described as Ping Pong Bi Bi Uni Uni (4) (see Appendix B), 2) separate catalytic subsites exist for the reactants of each partial reaction, 3) the two subsites are connected by a biotinyl residue that carries the carboxyl groups from one subsite to the other, 4) the mechanism of the Bi Bi partial reaction is a rapid equilibrium random (see Appendix B), and 5) substrate binding is relatively independent of the presence of acetyl-CoA, and the activating effect of the acyl-CoA is exerted on V_{\max} but has little effect on substrate K_m values. Feature 3) classifies the reaction as a "two-site Ping Pong mechanism" in contrast to the single-site mechanism common among transamination and transacylation enzymatic reactions.

Ligand Induced Conformational Transitions

Present theories concerning binding of substrates and allosteric effectors to enzymes propose linked conformational and binding equilibria. In fact, enzyme regulation by small molecular ligands is usually presumed to result from conformational transitions induced in the enzyme upon binding the ligand.

The changes in chicken liver pyruvate carboxylase produced by acetyl-CoA which lead to a catalytically active molecule would appear to involve conformational changes in the enzyme (1, 2, 3). Attempts to demonstrate such conformational changes by investigating variations in the enzyme's appearance in the electron microscope and measuring optical rotatory dispersion and protein fluorescence changes induced by acetyl-CoA have been unsuccessful. However, ultraviolet difference spectral studies show a small absorbance increase in the presence of acetyl-CoA with a peak at 280 nm and a second smaller peak at 288 nm. Also possible demonstration of a conformational change comes from the studies of the reacting forms of the yeast enzyme in the presence and absence of acetyl-CoA in the ultracentrifuge where the sedimentation coefficient of the reacting form is about 3% lower than it is in the presence of acetyl-CoA.

All the foregoing evidence is consistent with the view that any conformational transitions induced by the binding of acetyl-CoA to avian pyruvate carboxylase must be small. Aside from acetyl-CoA activation of the catalytic reaction itself, the most dramatic evidence for induced conformational changes has been the effect of acetyl-CoA on the rate of enzyme inactivation by avidin. Acetyl-CoA accelerates the rate

of inactivation, apparently by causing an enzyme conformational change that makes the biotin moiety much more susceptible to avidin. Conversely, ATP affords essentially complete protection against avidin inactivation, probably affecting the enzyme again in the vicinity of the biotin ring making it less susceptible. Avidin is a relatively large molecule (molecular weight = 68,000). A conformational change in the region of the active site sufficient to make the biotinyl-lysine residue available or unavailable to avidin may be a rather significant change; however, it may represent only a small difference in the gross structure of the protomer.

The objective of this study was to characterize possible conformational transitions in chicken liver pyruvate carboxylase, which are induced by acetyl-CoA, KHCO_3 , and MgATP binding, utilizing fluorescence probes and circular dichroism (in the presence and absence of fluorescent probes). Ideally to monitor conformational transitions, the fluorophore should be located at or near the active site. Fluorescent analogs of both MgATP and acetyl-CoA were used initially with no success. However, the fluorescent dye, 8-anilino-1-naphthalenesulfonic acid (ANS), responded nicely to addition of ligands. Many dyes like ANS bind noncovalently to macromolecules and often signal changes in the microenvironment of the bound dye due to perturbations caused by pH changes, small ligand binding, etc. Several investigators have demonstrated the utility of dyes as probes for conformational transitions in proteins induced by ligand binding (5, 6, 7).

As a further probe of conformational changes as well as the protein-ANS interaction, the far and near ultraviolet circular dichroism of pyruvate carboxylase has been studied in the presence and

absence of ANS and natural ligands (substrates and effector). The far ultraviolet (185-250 nm) contains spectral contributions of the peptide backbone and is a direct indication of the secondary structure of the protein. The near ultraviolet (240-310 nm) is dependent upon the tertiary and quaternary structure, since optical activity of the aromatic and cystine side chains may be induced by their presence in local asymmetric environments. This region may be sensitive to subtle alterations in protein conformation upon ligand binding. Small changes in the ultraviolet spectrum of pyruvate carboxylase upon addition of acetyl-CoA (as previously discussed) would tend to suggest possible changes in the circular dichroism spectra also. However, optical rotatory dispersion studies by Palacian and Neet (3) led us to believe that no variations in circular dichroism would be observed upon addition of acetyl-CoA in the presence (or absence) of ANS unless ANS was perturbing the enzyme into an unnatural form.

In summary, the objectives of this study were 1) to investigate possible conformational transitions induced by MgATP, acetyl-CoA, and KHCO_3 in chicken liver pyruvate carboxylase by fluorometric probes (ANS, ϵ -ATP, and ϵ -acetyl-CoA) and circular dichroic methods and 2) to gain an insight into the protein-ANS interaction and any deleterious effects ANS was inflicting on the native form and action of the enzyme. The latter study was necessary to assess the validity of results of the former study.

Secondary Structure Determination by Circular Dichroism

The far ultraviolet circular dichroism can be utilized in deter-

mining the percentages of helix, β -pleated sheet, and other structures (random coil, etc.) by the empirical method of Chen and Yang (8). The experimental mean residue ellipticity at wavelength λ is given by Equation (1-1)

$$[\theta]_{\lambda} = f_H[\theta]_{H,\lambda} + f_{\beta}[\theta]_{\beta,\lambda} + f_R[\theta]_{R,\lambda} \quad (1-1)$$

where $[\theta]_{H,\lambda}$, $[\theta]_{\beta,\lambda}$, and $[\theta]_{R,\lambda}$ are mean residue ellipticities of helix, β -pleated sheet, and random structures, respectively, and f_H , f_{β} , and f_R are the fractions of total protein in the corresponding structures. Random structures are defined as all conformations other than helix and β -pleated sheet. The mean residue ellipticities of each secondary structure type estimated from the five reference proteins of Chen and Yang (8) were used to estimate the secondary structure of pyruvate carboxylase from its far ultraviolet circular dichroism spectrum.

CHAPTER II

EXPERIMENTAL

Materials

Dithioerythritol (DTE), dithiothreitol (DDT), Trizma Base, phenylmethylsulfonylfluoride (PMSF), 5,5'-dithiobis-(2-nitrobenzoic acid) (DTNB), ATP, NADH, Coenzyme A (lithium salt), 8-anilino-1-naphthalene-sulfonic acid (ANS-magnesium salt), 2-mercaptoethanol, and ammonia color reagent (Nessler's Reagent) were from Sigma Chemical Company; EDTA and ultrapure $(\text{NH}_4)_2\text{SO}_4$ from Schwarz-Mann; oxaloacetate (sodium salt) from Calbiochem; pyruvic acid and D-10-camphor sulfonic acid from Aldrich; and 1,N⁶-ethenoadenosine 5'-triphosphate (ϵ -ATP) and (1,N⁶-etheno-) coenzyme A (ϵ -CoA-lithium salt) from P. L. Biochemicals, Inc. Pig heart malate dehydrogenase was purchased from Sigma; citrate synthetase from Boehringer; and crystalline bovine serum albumin from Pentex.

Other chemicals were reagent grade from Fisher Scientific. All reagents were dissolved in glass distilled water or buffers prepared with glass distilled water.

Methods

Miscellaneous Reagent Preparations

Magnesium chloride was further purified to remove heavy metals by

the method of Morrison and Uhr (9). Pyruvic acid was twice vacuum distilled and stored frozen as a 1 M solution. Upon dilution the pH of the acid was adjusted with KOH.

ANS was twice recrystallized from hot water, dried in a vacuum desiccator, and stored in the dark. Concentration in aqueous solution was determined at 350 nm with a molar absorptivity of $\epsilon = 4.95 \times 10^3 \text{ M}^{-1} \text{ cm}^{-1}$ (10).

Malate dehydrogenase was collected by centrifugation and sulfate removed by dialyzing against 3-4 changes (100 volumes each) of 10 mM potassium phosphate buffer, 1 mM EDTA, 8.58 mM MgCl_2 , 2 mM DTE, pH 7.6. A 0.1 M Tris-Cl buffer, 0.5 mM EDTA, 2 mM DTT, pH 7.9 was used in dialysis for the ϵ -ATP and ϵ -acetyl-CoA studies. Enzyme concentration ($\text{I.U./ml} = \mu\text{mole min}^{-1} \text{ ml}^{-1}$) was determined by spectrophotometric assay at 340 nm with 0.1 mM oxaloacetate and 0.2 mM NADH in the buffers specified above at 25°C.

Acetyl-CoA and ϵ -acetyl-CoA were prepared from LiCoA and acetic anhydride as suggested for acetyl-CoA by Frey and Utter (11), where acetic anhydride was limited to the amount necessary to give negligible unreacted coenzyme A (as determined with DTNB). Acetyl-CoA was enzymatically assayed with citrate synthetase by monitoring the release of coenzyme A with DTNB (12). Trizma Base was substituted for KHCO_3 in those preparations used in fluorescence experiments so that the effect of acetyl-CoA could be determined in the absence of KHCO_3 .

In fluorescence and circular dichroism measurements, ATP stock concentrations were calculated from spectrophotometric data assuming a molar absorptivity of $\epsilon = 15,400 \text{ M}^{-1} \text{ cm}^{-1}$ at 259 nm (13). The magnesium ion concentration was kept at least 4 mM in excess of ATP. Thus

ATP was present as MgATP and yet free Mg^{2+} was available to complex with the enzyme. At these levels of magnesium ion, phosphate concentrations were limited to 10 mM to avoid formation of precipitates.

Substrate and ANS solutions were prepared in buffers utilized in measurements and pH adjusted if necessary. All buffers for fluorescence were millipore filtered to remove dust.

Enzyme Preparation, Assay, and Protein

Determination

Pyruvate carboxylase was purified essentially by the procedure of Scrutton and Fung (14) from livers of 9-10 week old Cornish White Rock crossed chickens (usually starved 36 hours prior to sacrifice) and stored at pH 7.2 in 1.5 M sucrose, 0.025 M phosphate, 0.05 M $(NH_4)_2SO_4$, 1 mM EDTA, 2 mM DTE, and 2 μ M PMSF. A 1.5 hour dialysis against 3 liters of 0.025 M potassium phosphate buffer, 2 mM EDTA, 5 mM 2-mercaptoethanol, 2 μ M PMSF, pH 7.2 was substituted for the Sephadex G-25 column (11). Pyruvate carboxylase was assayed spectrophotometrically at 340 nm by coupling with malate dehydrogenase at 25°C. Except in early studies with the ϵ -derivatives the assay system contained 10 mM pyruvate, 2 mM ATP, 15 mM $KHCO_3$, 0.1 mM acetyl-CoA, 0.2 mM NADH, and approximately 5 I.U./ml malate dehydrogenase in 10 mM potassium phosphate buffer, 1 mM EDTA, 8.58 mM $MgCl_2$, 2 mM DTE, pH 7.6. The reaction was initiated by addition of pyruvate carboxylase. The assay system for studies with ϵ -ATP and ϵ -acetyl-CoA was 0.1 M Tris-Cl buffer, 0.5 mM EDTA, 8.35 mM $MgCl_2$, 2 mM DTT, pH 7.9 with other substrate concentrations as previously stated. Protein concentrations for fluorescence measurements were determined by the method of Kalckar (15) and

corrected by a factor of 2.0 (16). For circular dichroism measurements both the Kalckar and biuret methods using bovine serum albumin (17) as a standard were utilized, confirming the correction factor of 2.0. The ratio of extinction at 280 nm and 260 nm was approximately 1.5, a value characteristic of protein lacking bound nucleotide or other substances absorbing in this region. Pyruvate carboxylase concentrations were calculated on the basis of a molecular weight of 520,000 (3). Specific activities for all fluorescence and circular dichroism measurements were 13.5-15.5 I.U./mg and 17.8-18.7 I.U./mg, respectively.

Prior to use the purified enzyme was passed over a Sephadex G-50 (medium) column (1 cm x 25 cm or 0.3 cm x 6 cm depending on quantity) equilibrated with the buffer utilized in measurements at room temperature and eluted with the same buffer in order to remove sulfate which inhibits pyruvate carboxylase (14). Ammonium sulfate was located with Nessler's Reagent and was found to be eluted after the enzyme.

Pyruvate Carboxylase-ANS Fluorescence Studies

The buffer was 10 mM potassium phosphate, 1 mM EDTA, 8.58 mM $MgCl_2$, 2 mM DTE, pH 7.6 unless otherwise stated. The enzyme was stable in this buffer for at least 3 hours. In all fluorometric titrations a one ml sample of enzyme or enzyme-ANS was placed in a 1 cm pathlength quartz cuvette and aliquots of stock ligands added with a Hamilton microsyringe. Stock additives except ANS were prepared such that dilution effects were less than 2%. ANS stock (near the limit of its solubility) for enzyme-ANS dissociation constant (K_d) determinations gave a total dilution of 5%, and a correction for dilution was made.

The excitation and emission maxima of enzyme-ANS were 406 nm and

485 nm, respectively. All emission intensities were expressed in arbitrary fluorescence units or on a relative quenching basis, $(F_0 - F)/F_0$, where F_0 and F are fluorescence intensities before and after addition of ligands, respectively. Free ANS fluorescence was 2% or less of the protein bound ANS fluorescence at the protein and ANS concentrations utilized. All equilibrium and stopped-flow protein-ANS fluorescence measurements were done with enzyme greater than 90% saturated with ANS.

For stopped-flow measurements reactant solutions were deaerated 10 minutes at room temperature in a water aspirator vacuum system. At least 5 repetitions of a stopped-flow reaction were obtained for each solution condition.

Instrumentation

Assays were made in a Coleman 124 spectrophotometer equipped with a Coleman No. 0319 thermostatted cell holder, No. 801 scale expander, and No. 165 recorder at 25°C. Stopped-flow kinetic fluorescence measurements were made at 25°C in a Durrum-Gibson stopped-flow spectrophotometer equipped with a Durrum fluorescence accessory No. 16400, Durrum soft stop block No. 16647, xenon and tungsten sources, and Corning 3-72 filter with excitation at 406 nm and slit width of 2.0 mm. Fluorescence changes in a 1.82 cm pathlength stopped-flow cell were photographically recorded from a Tektronix storage oscilloscope. The deadtime under conditions utilized in most experiments was approximately 4 msec.

Investigation of equilibrium fluorescence changes induced by ligands on pyruvate carboxylase-ANS, tests for stability of ANS and

ANS-complexed enzyme upon prolonged irradiation, enzyme-ANS dissociation constant determination, and ϵ -derivative studies were performed at 25°C in a thermostatted Aminco-Bowman spectrophotofluorometer equipped with a xenon-mercury light source with a slit width of 3 mm.

Circular dichroism spectra were obtained on a Cary 61-CD model spectropolarimeter at 25°C in 1 mm and 1 cm pathlength cells for far and near ultraviolet regions, respectively. The optical path was flushed with nitrogen. The instrument was calibrated with an aqueous solution of D-10-camphor sulfonic acid using the molar ellipticity value determined by Cassim and Yang (18).

Data Analysis

For linear plots best straight lines were computed by a linear least squares method. The kinetic fluorescence data were converted by a CPS computer program to relative quenching as a function of time.

Nonlinear least squares fitting of Equation (3-2) (see Results and Discussion) was accomplished using the computer routine STEPIT (19) which seeks a local minimum of a smooth function of several parameters by a direct search method utilizing a chi-square estimate of the quality of fit (20). Standard deviations were calculated either by a linear approximation (21) or a support plane method. Data ordinates (relative quenching, RQ) were weighted by $[\sigma(RQ)]^{-2}$ where the standard deviation, σ , was estimated as approximately 2% calculated from the maximum precision in reading the photographic records. For fits to data with random error only, the expected value of chi-square is equal to the number of degrees of freedom (number of points - number of parameters). A chi-square equal to the number of degrees of freedom

corresponds to a 50% probability of obtaining a worse fit (chi-square probability = 0.5). A chi-square probability greater than approximately 0.1 is considered an acceptable fit by this criterion. Systematic errors of the same or greater magnitude result from instrumental and solution preparation errors. Thus probable errors of 2-3 times the computed standard deviations in parameters are expected.

Far ultraviolet data between 243 nm and 204 nm at 3 nm intervals were fit to Equation (1-1) using the minimization routine STEPIT (19) in conjunction with HELIX (22) which contained the reference set of $[\theta]_{H,\lambda}$, $[\theta]_{\beta,\lambda}$, and $[\theta]_{R,\lambda}$ of Chen and Yang (8). Standard deviation, σ , was estimated as approximately 5% of the measured $[\theta]_{\lambda}$. Computed error estimates were by the usual linear approximation (21).

CHAPTER III

RESULTS AND DISCUSSION

Fluorescence Probe Studies with ϵ -ATP and ϵ -Acetyl-CoA

With certain enzymes the biological activity of the adenosine-containing coenzymes is preserved to a considerable extent with the recently developed fluorescent ϵ -compounds (23). Under conditions where they act as substrates and effectors in substitution for the natural ligands, they are of great potential value. Being bound at the active site they can best monitor through their fluorescence, environmental changes (such as conformational transitions) in the vicinity of the active site.

To probe the usefulness of these derivatives, titrations of enzyme with ϵ -ATP and ϵ -acetyl-CoA were performed in 10 mM potassium phosphate buffer, 1 mM EDTA, 8.56 mM MgCl₂ (omitted with ϵ -acetyl-CoA titrations), 2 mM DTT, pH 7.0 at excitation 330 nm and emission 420 nm. Studies by North and Spivey (24) of this laboratory with pyruvate carboxylase suggested that the Tris-Cl buffer used in previous studies in this laboratory (25) was not ideal. Although fluorescence titrations of enzyme with ϵ -derivatives utilized a potassium phosphate buffer, enzyme assays were still being done at this time in Tris-Cl buffer. Maximum enzyme, ϵ -ATP, and ϵ -acetyl-CoA concentrations in titrations were

approximately 1.4 mg in 1.0 ml, 240 μ M, and 490 μ M, respectively.

Studies of pyruvate carboxylase with these derivatives, however, showed that the enzyme possessed no activity when ϵ -acetyl-CoA was substituted for acetyl-CoA and that the fluorescence of the derivative was unaffected by the presence of the enzyme. If binding occurred, it was in a nonproductive manner, and it induced no perturbation in the derivative's fluorescence.

Fluorescence quenchings of the order of experimental error (approximately 5%) were observed with ϵ -ATP. The validity of these changes was not further investigated because of their smallness.

Enzyme Stability and Catalytic Activity

Studies at Varying pH's

A buffer system containing 10 mM potassium phosphate, 1 mM EDTA, approximately 8.5 mM MgCl_2 , and 2 mM DTE was chosen for future enzyme measurements. In order to select a satisfactory pH, the enzyme's stability and enzymatic activity were determined in buffers over the range of pH 7.0-7.9.

The following buffer code is used below: 1) 10 mM potassium phosphate buffer, 1 mM EDTA, 8.37 mM MgCl_2 , 2 mM DTE, pH 7.0; 2) 10 mM potassium phosphate buffer, 1 mM EDTA, 8.45 mM MgCl_2 , 2 mM DTE, pH 7.2; 3) 10 mM potassium phosphate buffer, 1 mM EDTA, 8.52 mM MgCl_2 , 2 mM DTE, pH 7.4; 4) 10 mM potassium phosphate buffer, 1 mM EDTA, 8.58 mM MgCl_2 , 2 mM DTE, pH 7.6; and 5) 10 mM potassium phosphate buffer, 1 mM EDTA, 8.65 mM MgCl_2 , 2 mM DTE, pH 7.9.

Tests for enzyme stability in buffers 1, 3, and 5 were conducted by diluting and then assaying the enzyme over a 2 hour period in the

various buffers. A comparison of the degree of catalytic activity in buffers 1-5 was made by assaying the enzyme in these buffers and comparing initial velocities as a function of pH. The enzyme stock solution from which aliquots were taken to be used in the assays was prepared in 10 mM potassium phosphate buffer, 1 mM EDTA, 8.37 mM $MgCl_2$, 2 mM DTE, pH 7.0.

From stability and enzymatic activity measurements, 10 mM potassium phosphate buffer, 1 mM EDTA, 8.58 mM $MgCl_2$, 2 mM DTE, pH 7.6 was selected as the optimum buffer to be used in further measurements. The enzyme was stable over a 2 hour period at the pH's tested (7.0, 7.4, and 7.9). A plot of activity as a function of pH, presented in Figure 1, shows the pH optimum to be 7.6.

Equilibrium Pyruvate Carboxylase-ANS

Fluorescence Studies

Since the substrate-effector analogs, ϵ -ATP and ϵ -acetyl-CoA, showed no promise of successfully monitoring conformational changes, a second type of fluorescence probe, ANS, was investigated.

The addition of pyruvate carboxylase to a solution of ANS as indicated in Figure 2 results in approximately a 60-fold increase in fluorescence with negligible ANS or protein fluorescence relative to the protein-ANS fluorescence. Since free ANS shows an emission maximum at 515 nm, the characteristic blue shift is observed upon protein-ANS complexation (peak shift to 485 nm). At an excitation of 280 nm, the protein fluorescence is completely quenched under the conditions of Figure 2, indicating an energy transfer from the aromatic amino acid residues of the protein to the bound dye.

Figure 1. pH Optimum Determination. All buffers contained 10 mM potassium phosphate, 1 mM EDTA, and 2 mM DTE. $MgCl_2$ concentrations were 8.37 mM, 8.45 mM, 8.52 mM, 8.58 mM, and 8.65 mM at pH 7.0, 7.2, 7.4, 7.6, and 7.9, respectively. Pyruvate carboxylase dilution was made in 10 mM potassium phosphate buffer, 1 mM EDTA, 8.37 mM $MgCl_2$, 2 mM DTE, pH 7.0. Assays were performed at the substrate-effector levels previously described.

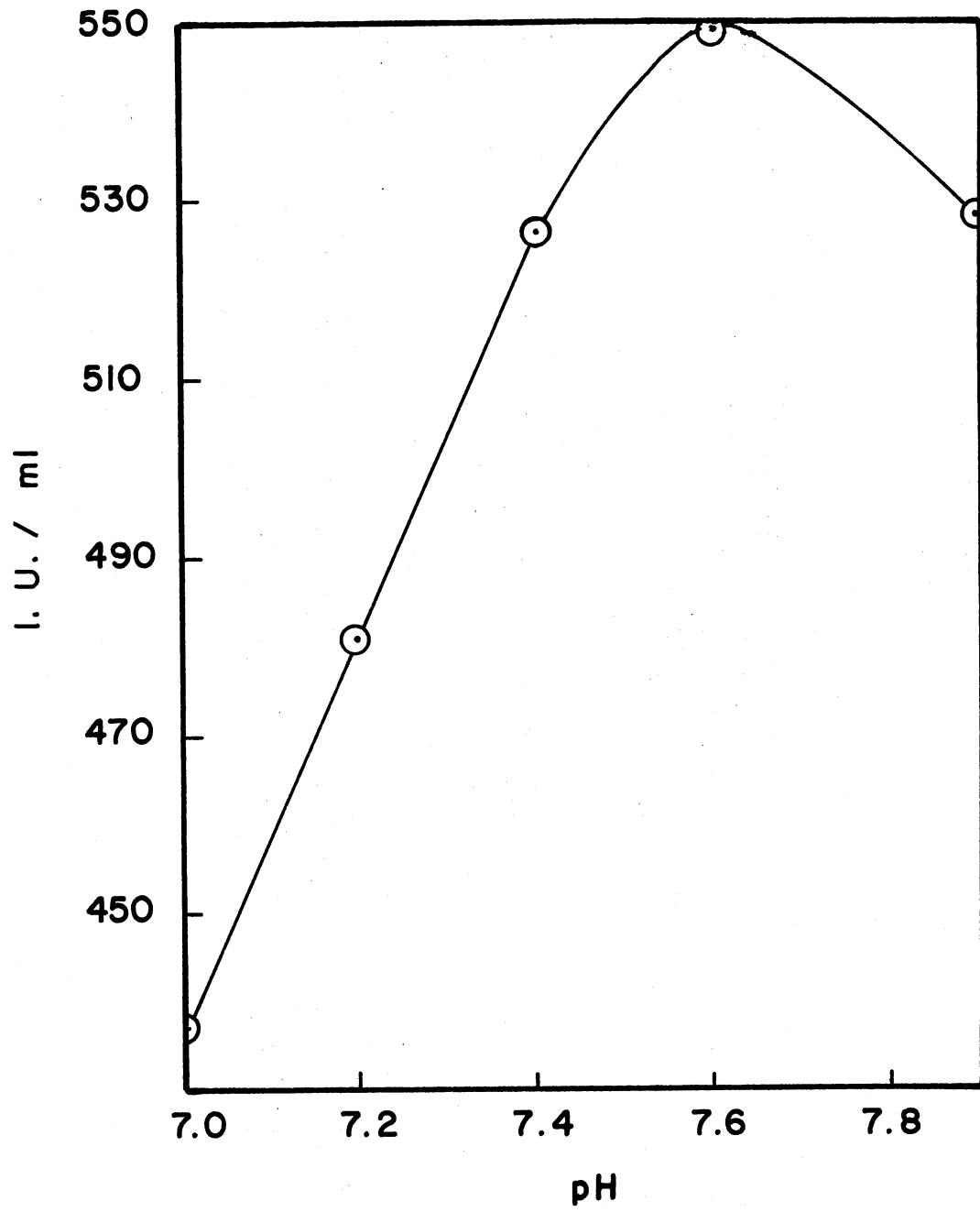
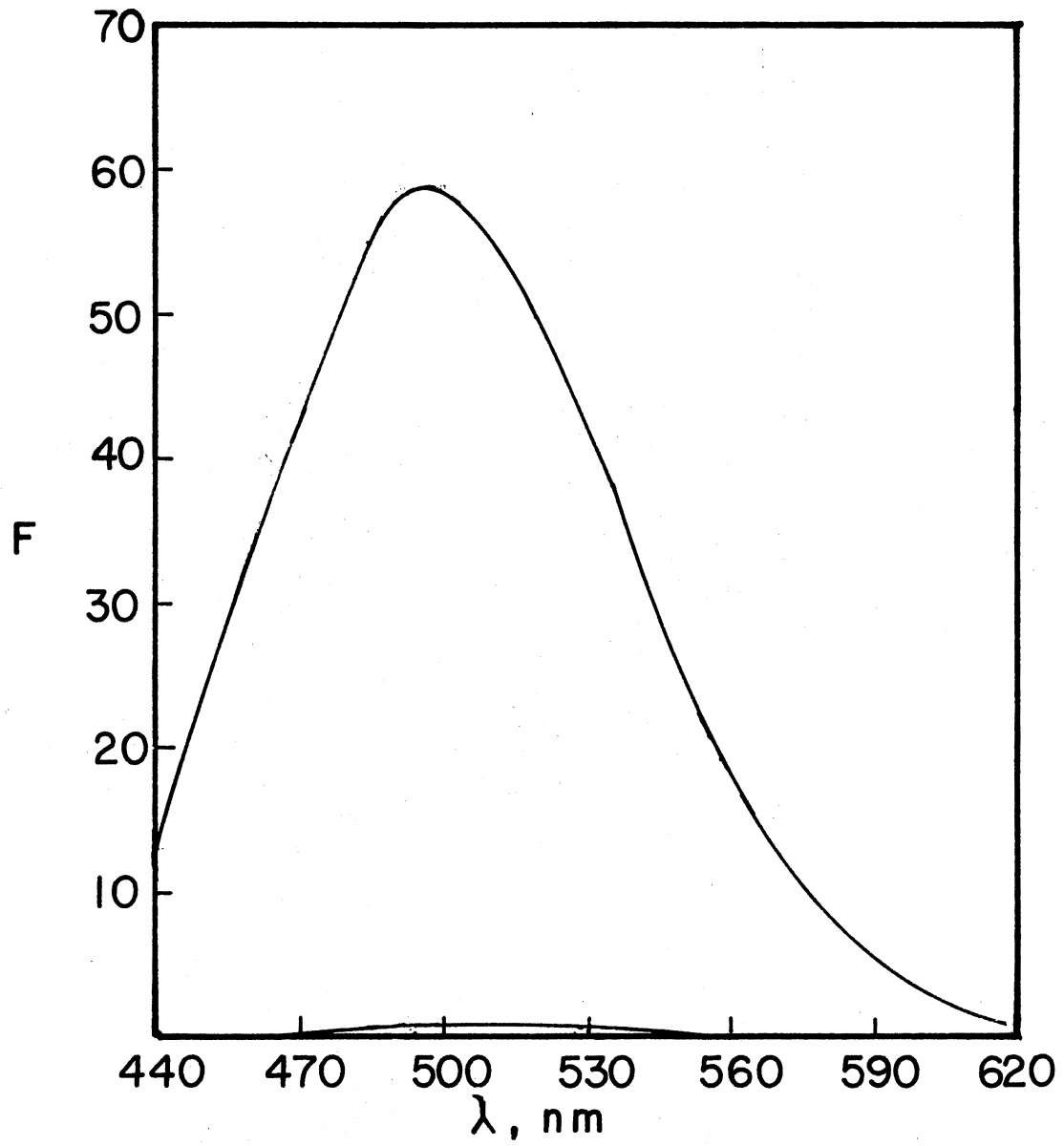


Figure 2. Fluorescence Spectra of ANS and ANS Bound to Pyruvate Carboxylase. For the pyruvate carboxylase-ANS spectrum (upper curve), a solution of 0.64 μ M pyruvate carboxylase (specific activity = 14.5 I.U./mg) and 0.32 mM ANS in 10 mM potassium phosphate buffer, 1 mM EDTA, 8.58 mM $MgCl_2$, 2 mM DTE, pH 7.6 was used. For the ANS spectrum (lower curve) the protein was omitted from the above solution. Fluorescence of free protein at this wavelength of excitation (406 nm) corresponded to the baseline. 25°C



The protein-ANS fluorescence (equilibrium measurements with Aminco-Bowman spectrophotofluorometer) was markedly quenched (Table I) by MgATP (21-24%) and acetyl-CoA (10-13%) with no significant change in the spectral position, suggesting that these ligands may produce a pronounced alteration in the environment of the bound ANS. Neither compound (MgATP or acetyl-CoA) has an absorption in either the excitation or emission region thus excluding an inner-filter mode of quenching. Nor do these species have any effect on the fluorescence of ANS in the absence of enzyme. KHCO_3 has no effect on the fluorescence of protein bound ANS. No detectable difference in final fluorescence values was observed with changes in the sequence of ligand addition, although rates of quenching were affected. The quenchings produced by acetyl-CoA and MgATP (in the presence of acetyl-CoA) were complete within the time of hand mixing (approximately 20 sec). The quenching by MgATP in the absence of acetyl-CoA extended over 5-10 minutes, although greater than 15% occurred within the time of hand mixing. The presence of acetyl-CoA did not affect the equilibrium magnitude of the MgATP quenching nor did KHCO_3 accelerate the MgATP effect in the absence of acetyl-CoA. Further aliquots of ligands produced no additional changes. The effects of individual substrates and effector at pH 7.0 (same buffer except 8.37 mM MgCl_2) were similar to the above measurements at pH 7.6; however, dependence of order and combinations was not tested.

Since increasing ionic strength (by addition of up to 0.072 M KCl) in the absence of ligands or in the presence of acetyl-CoA did not change the fluorescence of enzyme bound ANS, the fluorescence quenching was not ascribed to ionic strength changes caused by addition of ATP.

These studies were all performed in the presence of a Mg^{2+} containing buffer. Bais and Keech (7) with sheep kidney pyruvate carboxylase have reported a Mg^{2+} induced conformational change based on the alteration of the K_m values for MgATP in the presence of Mg^{2+} , entropy studies, and a quenching of the enzyme-ANS fluorescence by Mg^{2+} . In order to ascertain whether the change observed with ATP was caused by a decrease in free Mg^{2+} when ATP was added, the fluorescence intensities in the presence of 8.58 mM $MgCl_2$ (approximate free concentration of Mg^{2+} before 4.0 mM ATP is added) and 4.58 mM $MgCl_2$ (approximate free concentration of Mg^{2+} after 4.0 mM ATP is added) were compared. Based on the average of 3 separate determinations, the fluorescence intensities were identical at the two levels of Mg^{2+} . In the presence of 4.58 mM $MgCl_2$, $KHCO_3$, and acetyl-CoA showed identical effects to those previously described. If Mg^{2+} does affect the pyruvate carboxylase-ANS fluorescence, the effect occurs between 0-4.58 mM $MgCl_2$, which may be the case since Bais and Keech show that the quenching effect of Mg^{2+} is essentially complete at 0.4 mM Mg^{2+} . However, in the present case the decrease in free Mg^{2+} level as the ATP is added was not the explanation for the quenching.

In summary, the ligands MgATP and acetyl-CoA, but not $KHCO_3$, quench the fluorescence of the enzyme-ANS complex. These quenchantings are not ascribable to ionic strength changes or a decrease in free Mg^{2+} as ATP is added.

Dissociation Constant Determination for Enzyme-ANS Complex

The objective of this measurement was to gain insight into the

TABLE I
 DEPENDENCE OF FLUORESCENCE OF PYRUVATE
 CARBOXYLASE-ANS COMPLEX ON PRESENCE
 AND ORDER OF ADDITION OF ACETYL-
 CoA, ATP, AND KHCO₃

Addition Number ^a	Added species	[Added Species] mM	% Relative Quenching ^b
1	ATP	4.0	24
2	+ KHCO ₃ ^c	15.0	0
3	+ Acetyl-CoA	0.98	10
1	ATP	4.0	23
2	+ Acetyl-CoA	0.98	12
3	+ KHCO ₃	15.0	0
1	ATP	4.0	23
2	+ Acetyl-CoA, KHCO ₃ ^d	0.98, 15.0	12
1	ATP, Acetyl-CoA	4.0, 0.98	33
2	+ KHCO ₃	15.0	0
1	ATP, KHCO ₃	4.0, 15.0	22
2	+ Acetyl-CoA	0.98	12
1	Acetyl-CoA	0.95	13
2	+ KHCO ₃	15.0	0
3	+ ATP	4.0	21
1	Acetyl-CoA	0.95	13
2	+ ATP	4.0	21
3	+ KHCO ₃	15.0	0
1	Acetyl-CoA	0.95	12
2	+ KHCO ₃ , ATP	15.0, 4.0	21
1	Acetyl-CoA, KHCO ₃	0.95, 15.0	10
2	+ ATP	4.0	24
1	KHCO ₃	15.0	0
2	+ ATP	4.0	23
3	+ Acetyl-CoA	0.95	11
1	KHCO ₃	15.0	0
2	+ Acetyl-CoA	0.95	11
3	+ ATP	4.0	22

TABLE I (Continued)

1	KHCO ₃	15.0	0
2	+ Acetyl-CoA, ATP	0.95, 4.0	31
1	KHCO ₃ , Acetyl-CoA, ATP	15.0, 0.95, 4.0	33

^aPyruvate carboxylase was 0.45-0.52 μ M (specific activity = 14.4 I.U./mg). ANS concentration was 0.32 mM. Buffer was 10 mM potassium phosphate, 1 mM EDTA, 8.58 mM MgCl₂, 2 mM DTE, pH 7.6. Excitation was at 406 nm with emission at 485 nm. 25°C

^b% Relative Quenching = 100 X (F₀ - F)/F₀ where F₀ and F are fluorescence initially and after ligand addition, respectively. Before F was recorded the system was allowed to completely stabilize.

^cThe + represents addition to the previous solution.

^dAdded as a mixture with the concentration listing with respect to the substrate addition listing

enzyme-ANS interaction and the extent to which it was affected by the presence of MgATP and acetyl-CoA.

Data obtained from fluorescence titrations of pyruvate carboxylase with ANS in the absence and presence of MgATP or acetyl-CoA are given in Figure 3. From a plot of the fluorescence intensity, F , as a function of $F/[ANS]$ (Figure 4), estimates were obtained for the apparent dissociation constant, K_d , for the enzyme-ANS complex and the fluorescence maximum, F_{max} , that would be expected if the protein were fully saturated with the fluorophore. The mathematical analysis is formally identical with the Eadie plot (26). Determination of K_d by this method is outlined by Cheung and Morales (27) where $[ANS] \gg [Protein]$, and assumption is made that 1) each site binds ANS independently of the occupancy of other sites with apparent dissociation constant, K_d , and 2) the fluorescence per site is the same for every site.

Least squares values of K_d and F_{max} and their standard deviations were determined using Equation (3-1)

$$F = - K_d F / [ANS] + F_{max} \quad (3-1)$$

The linear plots obtained (Figure 4) support the conclusion that a single dissociation constant is being evaluated. K_d 's of $19.9 \pm 0.4 \mu M$, $19.5 \pm 0.1 \mu M$, and $19.2 \pm 0.2 \mu M$ were obtained in the absence of substrates, presence of MgATP, and presence of acetyl-CoA, respectively. These results indicate that MgATP and acetyl-CoA do not produce any significant change in the affinity of the enzyme for the fluorophore. This suggests that the observed decrease in F_{max} caused by MgATP and acetyl-CoA is caused by 1) decrease in number of hydrophobic binding sites for ANS on the enzyme as a result of ligand induced conformational

Figure 3. Effect of Varying ANS Concentrations on the Fluorescence of the Pyruvate Carboxylase-ANS Complex in the Presence and Absence of Acetyl-CoA and MgATP. Increasing concentrations of ANS were added to a solution of 0.72 μ M pyruvate carboxylase (specific activity = 14.6 I.U./mg) in 10 mM potassium phosphate buffer, 1 mM EDTA, 8.58 mM $MgCl_2$, 2 mM DTE, pH 7.6 in the absence of acetyl-CoA and MgATP, \bigcirc — \bigcirc ; presence of 4.0 mM ATP, \triangle — \triangle ; and presence of 0.1 mM acetyl-CoA, \square — \square . Correction has been made for dilution by ANS additions. Excitation was at 406 nm, and emission was at 485 nm.

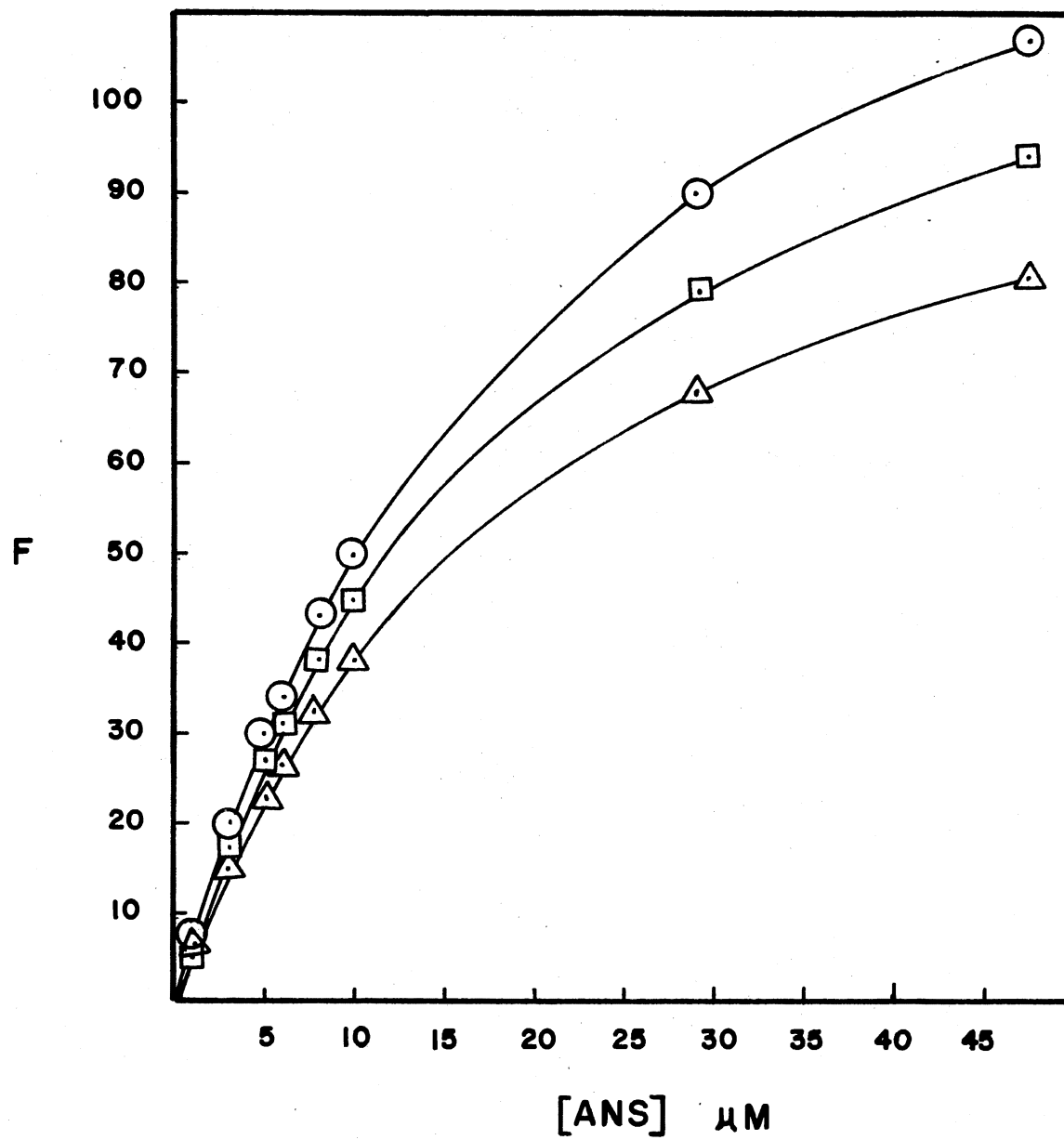
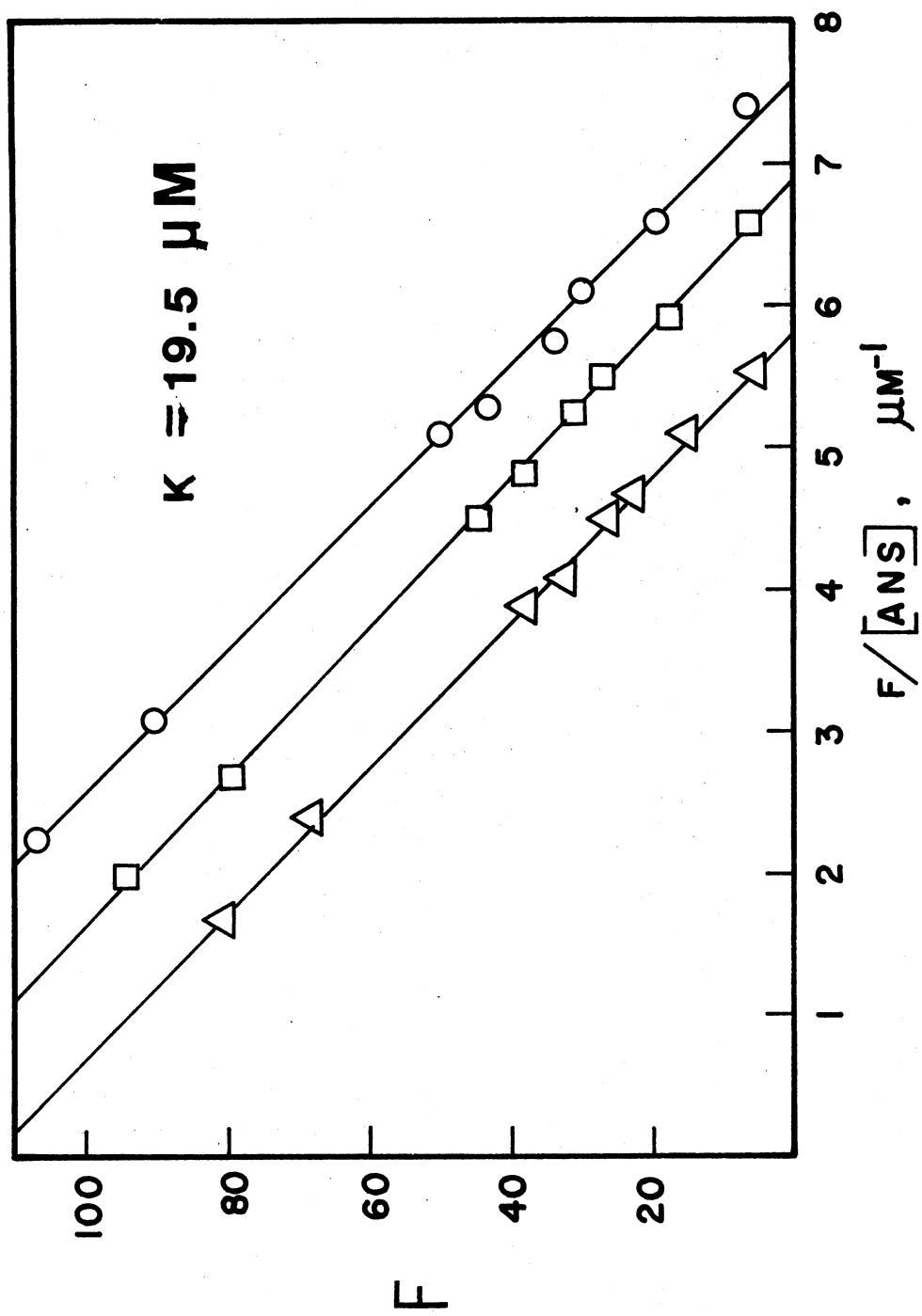


Figure 4. Replot of Data of Figure 3, Fluorescence as a Function of Fluorescence/[ANS].



change, 2) partial displacement of ANS by competitive binding of ligands, or 3) alteration in the polarity of the environment of bound ANS as a consequence of substrate induced conformational change with no change in the enzyme-ANS affinity. Constant K_d with altered F_{max} has also been reported by Aoe et al. (5) with fructose-1,6-diphosphatase and McClure and Edelman (28) with chymotrypsin who consider conformational alterations as the most probable explanation for their findings.

Effect of ANS on Pyruvate Carboxylase Activity

Since enzyme inactivation (29) as well as ANS induced kinetic inhibition (30) have been reported for other enzyme-ANS systems, the effect of ANS on the activity of pyruvate carboxylase was investigated. Solutions of pyruvate carboxylase (0.43-1.28 μ M) and ANS (0.46-7.68 mM) were incubated for 15 minutes and aliquots assayed in the presence of 2.3-92.1 μ M ANS. Controls were run in the absence of ANS.

No effects on enzyme activity could be observed over this wide range of assay conditions. Lack of inhibition indicates that ANS is not competing for the active site or causing detectable enzyme inactivation.

Kinetics of Pyruvate Carboxylase-ANS Binding

Further attempts to characterize the enzyme-ANS interaction were conducted by examining the binding of ANS to pyruvate carboxylase with stopped-flow methods. Transitions following the bimolecular binding step would indicate that the enzyme is converted to a nonnative conformation.

For stopped-flow measurements ANS (0.021-0.32 mM after mixing) was present in one syringe and enzyme (0.011-0.49 μ M after mixing) in the other. Measurements revealed that the enzyme-ANS complex formation is complete within the deadtime of the instrument (approximately 4 msec). No evidence of subsequent transitions following the bimolecular binding step was observed. Similar results have been found for transaldolase (6) and glutamate dehydrogenase (31); however, a slow first order process has been observed with bovine serum albumin (32) which indicates possible conversion to a nonnative form.

Kinetics of Ligand Induced Pyruvate Carboxylase- ANS Fluorescence Changes

In order to quantitate the rates of acetyl-CoA and MgATP induced enzyme-ANS fluorescence quenching, stopped-flow measurements were conducted. Table II summarizes the results of these studies under the conditions listed. The time course of the acetyl-CoA quenchings and acetyl-CoA accelerated MgATP changes observed in equilibrium fluorescence measurements were too rapid to be observed by the stopped-flow method also. The equilibrium values were entirely consistent with those obtained in non-stopped-flow measurements. Typical progress curves for the MgATP fluorescence quenching in the absence of acetyl-CoA are shown in Figure 5 for 3 enzyme and 3 ATP concentrations. Measurements were performed under pseudo first order conditions, $[ATP] \gg [Enzyme]$. Each curve possesses three phases. The slower phases are not due to photodecomposition of the complexed enzyme-ANS or ANS, since irradiation for over 15 minutes produced no detectable fluorescence changes. Under the stopped-flow drive pressure conditions

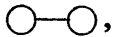
TABLE II
STOPPED-FLOW KINETICS MEASUREMENTS

Contents of Syringe 1 ^a	Contents of Syringe 2 ^a	% Relative Quenching ^{b,c}
0.48 μ M Enzyme 0.32 mM ANS	0.10 mM Acetyl-CoA	11% - unobservably rapid
0.48 μ M Enzyme 0.32 mM ANS	0.10 mM Acetyl-CoA 4.0 mM ATP	35% - unobservably rapid
0.48 μ M Enzyme 0.32 mM ANS 0.10 mM Acetyl-CoA	4.0 mM ATP	35% - unobservably rapid
0.51-1.65 μ M Enzyme 0.32 mM ANS	0.1-4.0 mM ATP	11-24% - 3 phase change

^aThese are after mixing concentrations.

^bSpecific activity of pyruvate carboxylase = 13.5-15.3 I.U./mg. Buffer was 10 mM potassium phosphate, 1 mM EDTA, 8.58 mM MgCl₂, 2 mM DTE, pH 7.6.

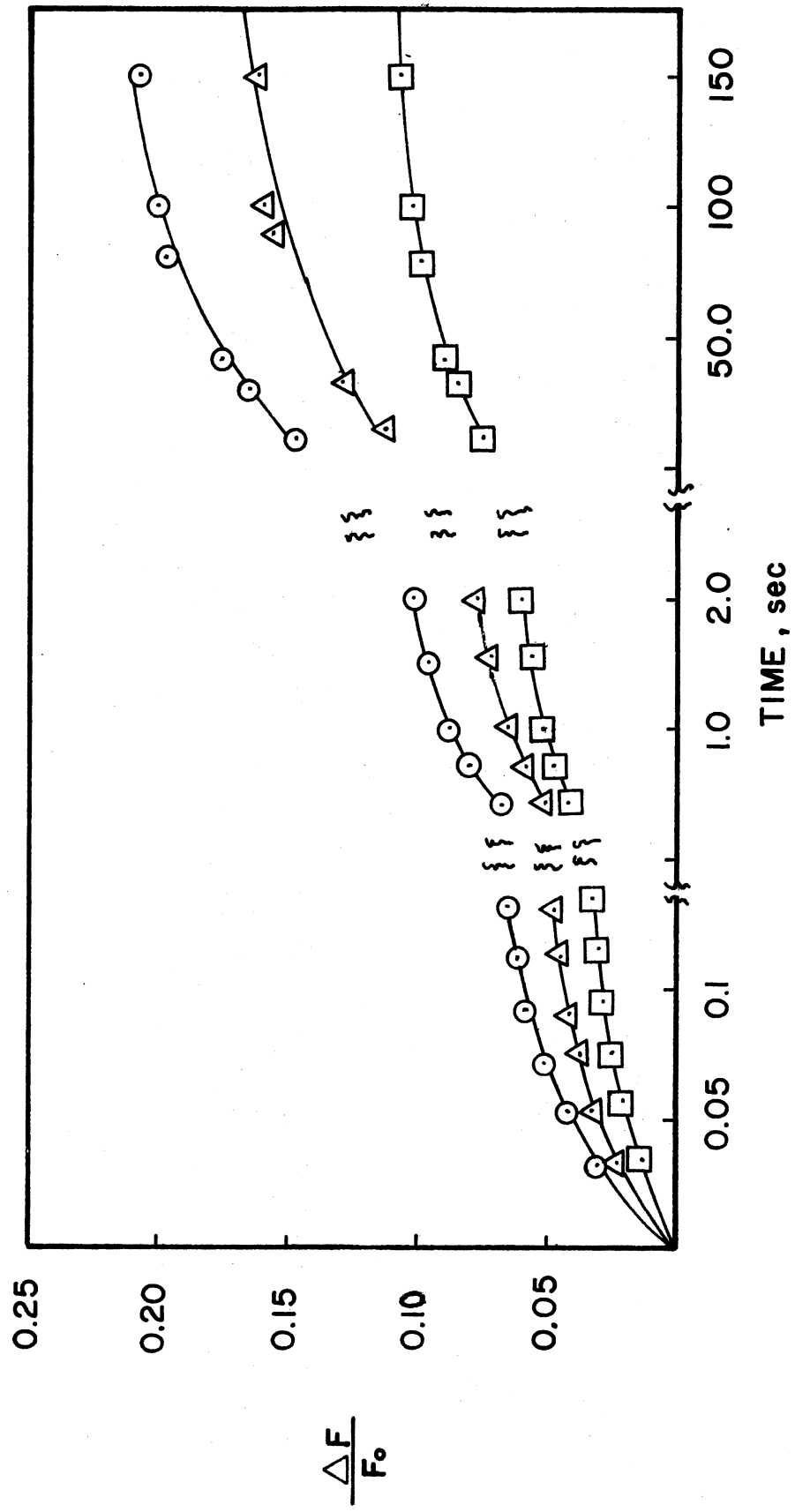
^c% Relative Quenching = $(F_0 - F)/F_0 \times 100$, where F_0 and F are initial and final (equilibrium) fluorescence, respectively.

utilized, only an estimated 0.4% quenching occurred within the instrument deadtime. Thus the initial fluorescence quenching recorded at time = 4 msec was taken to be the initial fluorescence. That essentially the complete progress curve is being observed is also substantiated by comparison of the equilibrium magnitude of the quenching observed in the stopped-flow measurement and in the previous equilibrium measurement (Aminco-Bowman spectrophotofluorometer). Within the expected experimental error, the same progress curve corresponding to conditions of curve , Figure 5 was observed when the drive pressure was reduced by half, although a small correction in the initial fluorescence was necessary due to the increased deadtime of the instrument. When pyruvate carboxylase-ANS was mixed in the stopped-flow instrument with buffer (no ATP), no change in fluorescence was observed indicating no perturbation of the enzyme-ANS fluorescence after the deadtime because of dilution or instrument stress on the complex. Assays of the enzyme before and after stopped-flow experiments (sample from stopped-flow cuvette) gave activities within 10% of each other, further confirming that the stopped-flow system induced no irreversible effects on the enzyme.

The progress curves were represented by a sum of exponentials. Fits to a sum of two exponentials gave unreasonably large chi-square values (χ^2 probability $\ll 0.5$) indicating a poor representation of the data by the chi-square criterion of goodness of fit. However, satisfactory fit ($\chi^2 \geq 0.5$) to Equation (3-2), a sum of three exponentials, was obtained where F_0 and F_t are fluorescence observed initially and at

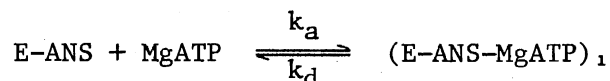
$$(F_0 - F_t)/F_0 = A_2 + A_3 + A_4 - (A_2)e^{-\lambda_2 t} - (A_3)e^{-\lambda_3 t} - (A_4)e^{-\lambda_4 t} \quad (3-2)$$

Figure 5. Progress Curves for the Reaction of Pyruvate Carboxylase-ANS with MgATP for Various Enzyme and MgATP Concentrations. Buffer was 10 mM potassium phosphate, 1 mM EDTA, 8.58 mM $MgCl_2$, 2 mM DTE, pH 7.6. ANS concentration was 0.32 mM. Enzyme specific activity was 13.5-15.3 I.U./mg. Pyruvate carboxylase and ATP concentrations were respectively: 0.51-0.55 μM and 4.0 mM, $\circ-\circ$; 1.0 μM and 4.0 mM, $\circ-\circ$; 1.65 μM and 4.0 mM, $\circ-\circ$; 0.51-0.55 μM and 0.34 mM, $\triangle-\triangle$; and 0.51-0.55 μM and 0.10 mM, $\square-\square$. 25°C, 1.82 cm pathlength stopped-flow cuvette, 406 nm excitation

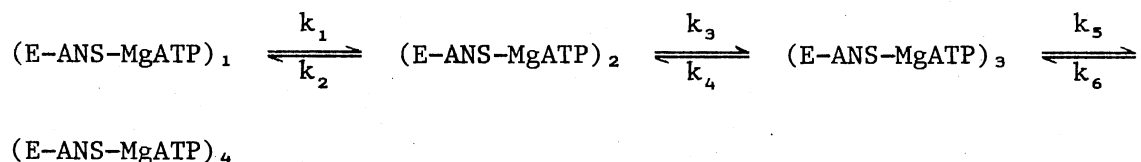


time t , respectively; A_2 , A_3 , and A_4 are pre-exponential or amplitude parameters; and λ_2 , λ_3 , and λ_4 are exponential or time parameters. The fitted values of these parameters are tabulated in Table III. Systematic errors of 2-3 times the random error are probable. Within expected errors, amplitude factors show no apparent dependence on enzyme concentration but a substantial ATP dependence. No apparent enzyme or ATP dependence is shown in the time constants.

With three exponentials no less than three transitions must be occurring. The following mechanism is proposed based on 1) known models of enzymatic transitions which would predict a bimolecular binding step of substrate to enzyme followed by possible unimolecular transitions, 2) conclusions by past investigators (3) that the binding of reactants to the enzyme in the Bi Bi partial reaction is described by a rapid equilibrium mechanism, and 3) the present experimental results with the enzyme-ANS complex. In the proposed mechanism, substrate binds in a rapid equilibrium binding step



followed by several unimolecular transitions



where E represents the native enzyme.

Our kinetic treatment of this mechanism (See Appendix A) includes the following assumptions: 1) Initial establishment of equilibrium in the rapid equilibrium binding step occurs before our observation of the reaction on the oscilloscope. This assumption necessitates that the

TABLE III
 KINETIC BEST FIT VALUES OF EQUATION (3-2)
 PARAMETERS FOR MgATP INDUCED
 CHANGES IN ENZYME-ANS
 FLUORESCENCE

[Enzyme] ^a μM	[ATP] mM	Parameters					
		A2 X 10 ²	A3 X 10 ²	A4 X 10 ²	λ ₂ X 10 ⁻¹ sec ⁻¹	λ ₃ X 10 ⁻¹ sec ⁻¹	λ ₄ X 10 ² sec ⁻¹
0.51-0.55	0.10	3.4 + 0.04 ^b - 0.05	3.8 + 0.08 - 0.2	4.4 + 0.1 - 0.08	1.5 + 0.03 - 0.03	5.5 + 0.5 - 0.2	1.1 + 0.09 - 0.05
0.51-0.55	0.34	5.1 ± 0.1	5.7 ± 0.2	6.9 ± 0.2	1.8 ± 0.06	6.0 ± 0.4	1.1 ± 0.07
0.51-0.55	4.0	6.8 ± 0.08	7.2 ± 0.2	8.6 ± 0.2	1.7 ± 0.03	5.3 ± 0.3	1.1 ± 0.07
1.01	4.0	6.8 ± 0.08	7.3 ± 0.2	8.5 ± 0.2	1.7 ± 0.03	5.2 ± 0.3	1.1 ± 0.06
1.65	4.0	6.9 ± 0.03	7.2 ± 0.07	8.5 ± 0.08	1.6 ± 0.02	5.1 ± 0.1	1.1 ± 0.03

^aSpecific activity of pyruvate carboxylase = 13.5-15.3 I.U./mg. Buffer was 10 mM potassium phosphate, 1 mM EDTA, 2 mM DTE, 8.58 mM MgCl₂, pH 7.6. ANS concentration was 0.32 mM. 25°C

^bError from a support plane method rather than a linear approximation

fluorescence emissivities of E-ANS and (E-ANS-MgATP)₁ are identical, since the entire quenching process is observed. Justifications for this assumption are the following: a) The half-life, $t_{1/2}$, for substrate binding to enzymes under conditions of 4 mM MgATP may be as fast as 10^{-6} sec if MgATP is acting as a "good" substrate. Based only on observations with other enzymes, this is not a rigorous justification for assumption 1). b) No dependence on MgATP concentration is shown by the time constants. c) If the initial equilibrium establishment in the bimolecular step were observed, the ratio of initial slopes $(\Delta F/\Delta t)_{4.0 \text{ mM}} / (\Delta F/\Delta t)_{0.1 \text{ mM}}$ should be 40 (at constant enzyme-ANS concentration). Experimentally, it is 2. 2) Since $\lambda_3 \gg \lambda_4$ (from least squares fits), the last transition can be adequately uncoupled for times less than approximately 7 sec.

Solution of differential equations describing the remaining four enzyme containing species yields expressions of the following form (see Appendix A)

$$[\text{E-species}] = a_1 e^{-\lambda_2 t} + a_2 e^{-\lambda_3 t} + a_3$$

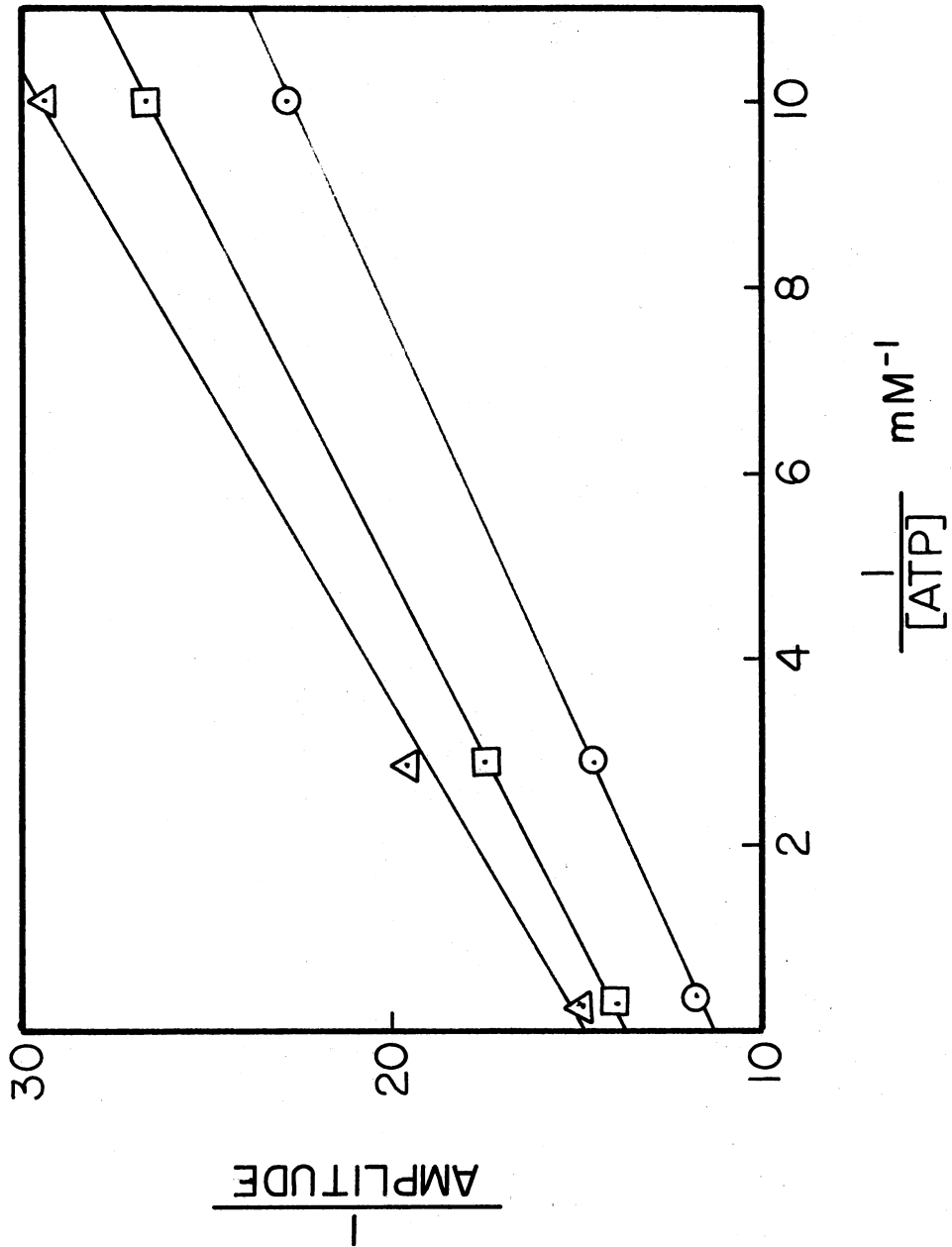
where λ_2 , λ_3 , a_1 , a_2 , and a_3 are constants (at fixed total enzyme concentration and fixed MgATP concentration). The time constants, λ_2 and λ_3 , are the same for every enzyme species, and a_1 , a_2 , and a_3 vary from species to species. When the expressions for each enzyme species together with unknown fluorescence emissivities are substituted into the mathematical expression for relative quenching, the final equation is of the form (see Appendix A)

$$(F_0 - F_t)/F_0 = A_2 + A_3 - (A_2)e^{-\lambda_2 t} - (A_3)e^{-\lambda_3 t}$$

where the constants A2 and A3 contain unknown rate constants, unknown fluorescence emissivities, and the substrate dependence. The fitted equation (Equation (3-2)) is generated from this expression upon adding the third exponential for the last transition (which had been previously uncoupled). Since the fluorescence change is normalized by the initial fluorescence (which depends on $[E]_t$, the total enzyme concentration), the enzyme concentration should not appear as a pre-exponential dependence, in agreement with experimental observations. As the mechanism would predict, experimentally the time constants show no enzyme concentration dependence. Both time and pre-exponential factors contain terms which depend on ATP concentration. For this mechanism to be valid, the absence of an observable ATP dependence in experimental time constants requires that the single ATP (denoted as $[S]_t$ in Appendix A) dependent term in the λ expressions (see Equation (A-6) in Appendix A) is small relative to the other terms.

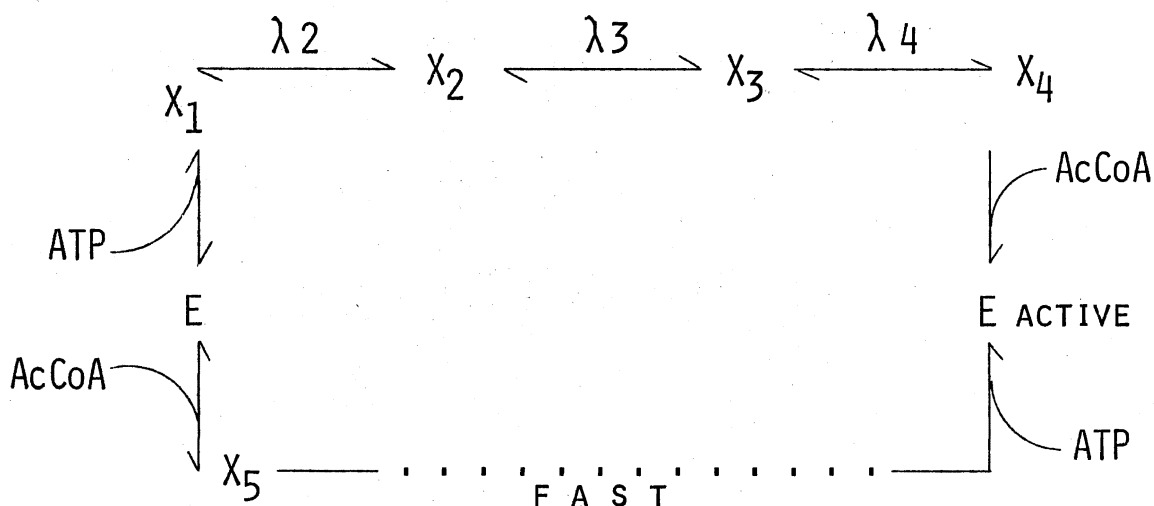
All experimental pre-exponential factors are rectangular hyperbolic functions of ATP concentration as shown by reciprocal plots in Figure 6. If the general form for a rectangular hyperbola is $(a[\text{ATP}]) / (1 + b[\text{ATP}])$ where a and b are constants, then least squares analysis of the data of Figure 6 gives b values of 10.0, 10.4, and 9.9 mM^{-1} for the A2, A3, and A4 plots, respectively. Thus the rectangular hyperbolas generated by the pre-exponential factors of Equation (3-2) differ only in the amplitude factor, a . If A2, A3, and A4 are averaged for the three enzyme concentrations utilized at the 4.0 mM ATP level, negligibly different b values are obtained. Kinetic analysis of the proposed mechanism (using the uncoupled system in Appendix A) suggests that the pre-exponential factors should be expressions containing three types of

Figure 6. Double Reciprocal Plots of Best Fit Values of A2, A3, and A4 (Amplitude Parameters in Equation (3-2)) as a Function of ATP Concentration. Buffer was 10 mM potassium phosphate, 1 mM EDTA, 8.58 mM MgCl₂, 2 mM DTE, pH 7.6. Pyruvate Carboxylase concentration was 0.51-0.55 μM (specific activity = 13.5-15.3 I.U./mg). ANS concentration was 0.32 mM. Curves correspond to 1/A2 versus 1/[ATP], \triangle - \triangle ; 1/A3 versus 1/[ATP], \square - \square ; and 1/A4 versus 1/[ATP], \circ - \circ . 25°C



terms, two of which are rectangular hyperbolas. Not knowing the relative magnitudes of these terms, it is impossible to predict whether one type of term should mask the others and whether these experimental data precisely fit the mechanism. Since the eight forward and reverse rate constants and fluorescence emissivities of the five enzyme-ANS species are unknown, no further analysis of this system has been attempted.

Based on the foregoing observations the following scheme of transitions upon binding of acetyl-CoA and MgATP is proposed. These transitions are consistent with popular theories of allosteric regulation and reveal the conformational adaptability that appears to be a general and requisite feature of enzyme catalytic mechanisms. Whether the enzyme exists in the same final conformation irrespective of the order of ligand additions is debatable. The sole argument for the same final state is the identical final magnitude of quenching despite the order of addition. If the same final state is indeed achieved, acetyl-CoA must act to facilitate the MgATP change, since the MgATP change is greatly accelerated in the presence of acetyl-CoA.



Changes in Circular Dichroism of Pyruvate
Carboxylase Induced by ANS, MgATP,
and Acetyl-CoA

To strengthen conclusions based on fluorescence studies, the far and near ultraviolet spectra of native and ANS-complexed pyruvate carboxylase were compared in the presence and absence of MgATP and acetyl-CoA. Free ANS is optically inactive; however, Daniel and Yang (33) have reported induced circular dichroism in ANS upon binding to bovine serum albumin. It is possible that a protein circular dichroism spectrum may be altered by an optically inactive binding ligand (that is, optically inactive in the absence of the protein) for several reasons: 1) induced circular dichroism in the ligand due to its presence in an asymmetric environment without any change in the structure or conformation of the protein, 2) a structural change in the enzyme induced by the ligand's presence without causing a change in the optical activity of the ligand, or 3) a combination of these two factors.

The buffer system utilized in the measurements was 10 mM potassium phosphate, 8.58 mM MgCl₂, pH 7.6. Total dilution effects of successive ligand additions to the enzyme solution were 5% maximum, and a dilution correction was made in the quoted mean residue ellipticities. The spectra obtained in the presence of acetyl-CoA and/or MgATP were corrected by subtracting background acetyl-CoA and/or MgATP spectra, since acetyl-CoA and ATP ligands exhibit intrinsic circular dichroism. A mean residue molecular weight of 118 was used in all mean residue ellipticity calculations. Consecutive scans of the same solution were

quite reproducible in the far ultraviolet (approximately 2% variation) and fairly reproducible in the 285-350 nm range (approximately 5% variation).

No discernible difference in the far (0.38-0.41 μM enzyme) and near (5.8 μM enzyme) ultraviolet spectra was produced by the presence of 0.1 mM ANS, indicating that ANS is not inducing gross changes in the protein structure (in agreement with indications from earlier activity studies). The difference spectra (protein or protein-ANS with acetyl-CoA and/or MgATP spectrum minus acetyl-CoA and/or MgATP spectrum) in the far ultraviolet showed no detectable difference from the protein and protein-ANS spectra, indicating no gross ligand induced changes in the protein secondary structure. Figures 7 and 8 show typical near and far ultraviolet spectra, respectively. Table IV is a compilation of ligand induced changes observed in the near ultraviolet 292 nm and 285 nm peaks. As is indicated the changes induced by MgATP and acetyl-CoA in the absence of ANS are maintained in its presence. This tends to confirm that ANS is not interfering with substrate induced changes and acts merely as a monitor of these changes. MgATP decreases both the 292 nm and 285 nm peaks. Acetyl-CoA increases both peaks. The final $\theta_{292}/\theta_{285}$ and $[\theta]_{292}$ values after addition of MgATP and acetyl-CoA are essentially the same irrespective of order of addition, similar to the independence of fluorescence change on order of addition. It is not possible to know with certainty the explanation for these near ultraviolet changes. Even though the intrinsic circular dichroism of MgATP and acetyl-CoA is subtracted from the protein (or protein-ANS)-ligand circular dichroism at each wavelength, perhaps the intrinsic circular dichroism of MgATP and/or acetyl-CoA is changed upon binding to the

Figure 7. Near Ultraviolet Pyruvate Carboxylase Circular Dichroism Spectrum. Buffer was 10 mM potassium phosphate, 8.58 mM $MgCl_2$, pH 7.6. Enzyme concentration was 1.5 mg/ml (specific activity = 17.8 I.U./mg), 1 cm pathlength cuvette, 25°C

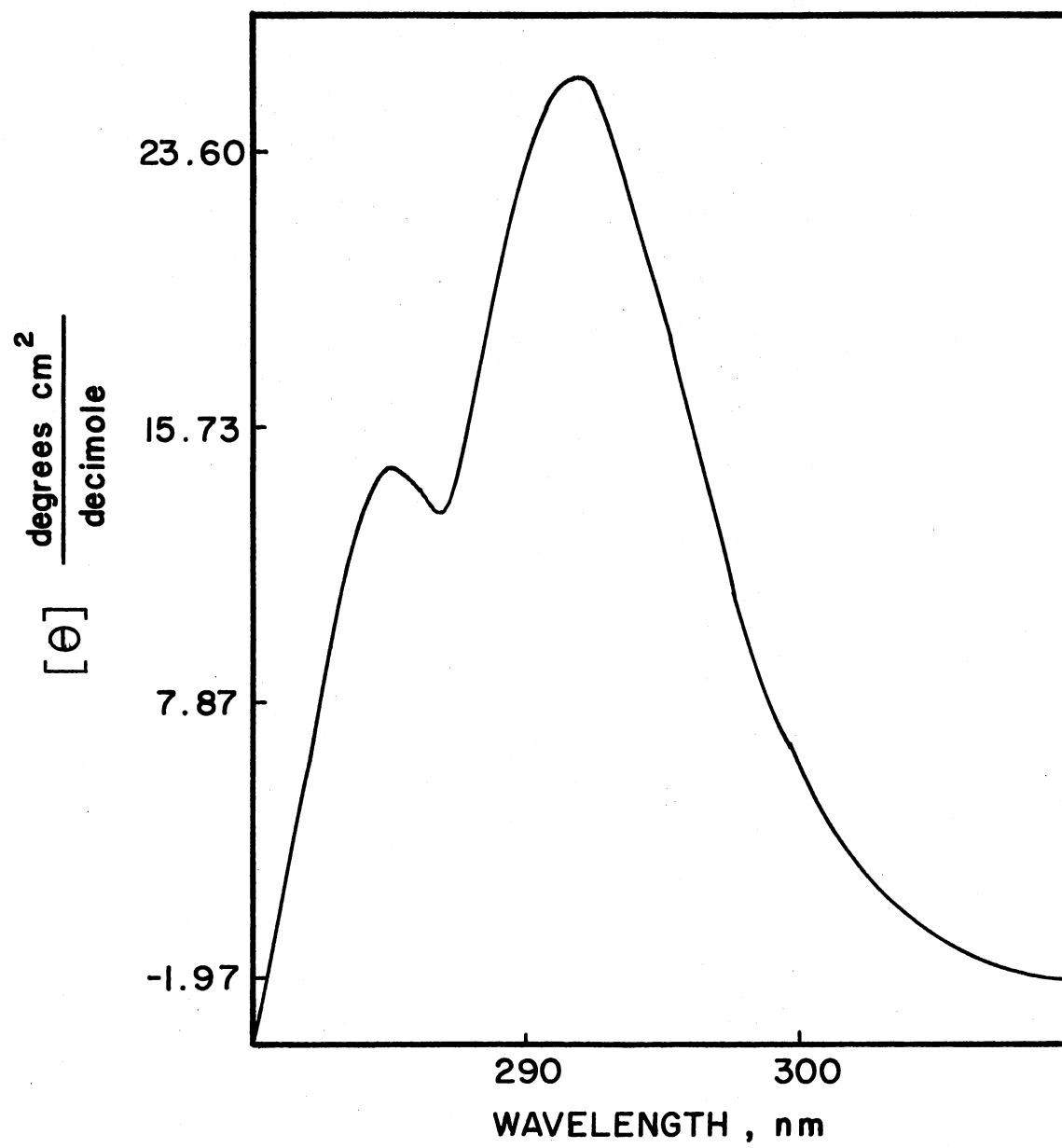


Figure 8. Far Ultraviolet Pyruvate Carboxylase Circular Dichroism Spectrum. Buffer was 10 mM potassium phosphate, 8.58 mM $MgCl_2$, pH 7.6. Enzyme concentration was 0.10 mg/ml (specific activity = 18.7 I.U./mg). Fitted values obtained using the empirical method of Chen and Yang (8) and experimental values are denoted by \bigcirc and — , respectively. 1 mm cuvette, 25°C

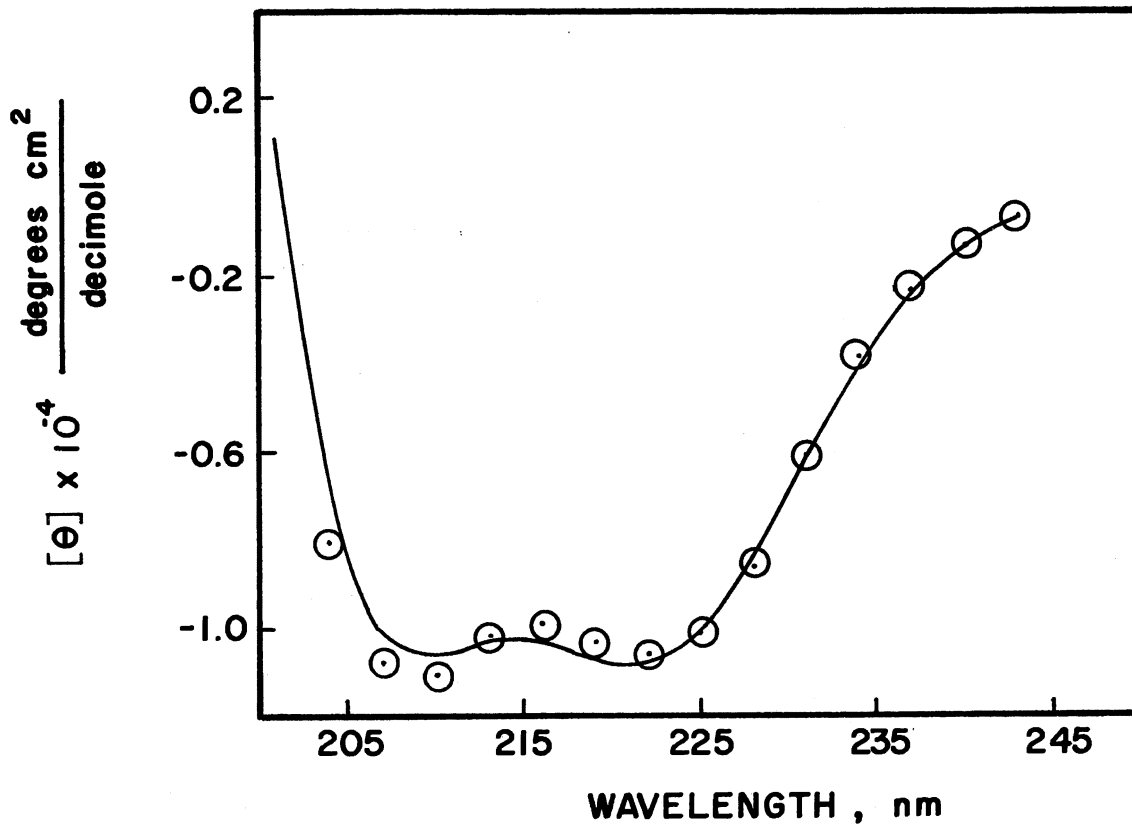


TABLE IV

EFFECT OF MgATP AND ACETYL-CoA ON PYRUVATE
 CARBOXYLASE AND PYRUVATE CARBOXYLASE-ANS
 292 NM AND 285 NM CIRCULAR
 DICHROISM PEAKS

Data Set Number ^a	[ANS] mM	[ATP] mM	[Acetyl-CoA] mM	λ nm	$\frac{\theta_{292}}{\theta_{285}}$	$[\theta]_{\lambda}^c$ ± 1.0
1 ^b	-----	-----	-----	292 285	1.8	26 15
	-----	-----	0.096	292 285	1.5	29 19
	-----	0.97	0.094	292 285	2.4	26 11
2	-----	-----	-----	292 285	1.7	26 15
	0.10	-----	-----	292 285	1.7	26 15
	0.10	-----	0.095	292 285	1.5	29 19
	0.097	0.96	0.093	292 285	2.4	27 11
3 ^b	-----	-----	-----	292 285	1.7	25 15
	-----	0.98	-----	292 285	2.5	24 9
	-----	0.97	0.094	292 285	2.4	27 11
4	-----	-----	-----	292 285	1.8	26 14
	0.10	-----	-----	292 285	1.8	25 14
	0.098	0.97	-----	292 285	2.5	24 9

TABLE IV (Continued)

0.097	0.96	0.093	292	2.4	26
			285		11

^aInitial pyruvate carboxylase concentration was 3.0 mg/ml. Specific activity = 17.8 I.U./mg. Buffer was 10 mM potassium phosphate, 8.58 mM MgCl₂, pH 7.6. 25°C

^bAverage of two determinations

^cValues are corrected for enzyme dilution as additions were made to the enzyme solution. Units are degree-cm² per decimole.

protein, and the change reported is not caused by tertiary structure changes in the protein. However, the fluorescence changes certainly support the conclusion that optical activity changes are also the result of conformation changes. At the very least the same circular dichroism changes are occurring in the presence and absence of ANS, indicating no gross enzyme change upon binding of ANS.

Secondary Structure Estimation Utilizing Far Ultraviolet Circular Dichroism

The fitted values for secondary structure types were $27.3 \pm 0.6\%$ helix and $6.6 \pm 0.9\%$ β -pleated sheet. The experimental spectrum with fitted points is shown in Figure 8. The chi-square value for the fitted curve is 33 compared to a theoretical 12 degrees of freedom indicating only a fair fit (χ^2 probability < 0.1). To improve chi-square would require σ to be greater than $5\% \times [\theta]_{\lambda}$, which is an unrealistic estimate of σ . Inexactness in the model probably accounts for the quality of fit.

The helical estimate will be high or low according to how well the average helical lengths of pyruvate carboxylase agree with the overall helical lengths of the chosen reference proteins (34). If the average helical length in pyruvate carboxylase is greater than that of the reference set, the computed fraction of helix will be overestimated and vice versa. It is difficult to assess the validity of these secondary structure estimates except that they are reasonable values for proteins in general.

CHAPTER IV

SUMMARY AND CONCLUSION

This study demonstrates the utility of the fluorescence probe ANS with pyruvate carboxylase. All evidence is consistent with the conclusion that MgATP and acetyl-CoA induce conformational changes in the enzyme. To so successfully monitor environmental changes induced by these ligands, the probe must be situated at a crucial position on the enzyme. And of special importance is the indication that the probe is not deleterious to the enzyme's native form. In particular, experiments to further characterize the conformational transitions induced by acetyl-CoA are suggested by the success of this system. These include relating equilibrium extents of conformational changes with the acetyl-CoA binding function which can be diagnostic of the allosteric mechanism and temperature jump relaxation measurements which are sufficiently fast to record the rates of acetyl-CoA activation.

A SELECTED BIBLIOGRAPHY

- (1) Utter, M. F. and Scrutton, M. C. (1969) in Current Topics in Cellular Regulation, B. L. Horecker and E. Stadtman, eds., Vol. 1, pp. 253-296. Academic Press, New York.
- (2) Scrutton, M. C. and Young, M. R. (1972) in The Enzymes, P. D. Boyer, ed., Vol. VI, pp. 1-35. Academic Press, New York.
- (3) Utter, M. F., Barden, R. E., and Taylor, B. L. (1975) in Advances in Enzymology, A. Meister, ed., Vol. 42, pp. 1-72. John Wiley and Sons, New York.
- (4) Cleland, W. W. (1963) Biochim. Biophys. Acta, 67, 104-137.
- (5) Aoe, H., Sarngadharan, M. G., and Pogell, B. M. (1970) J. Biol. Chem., 245, 6383-6387.
- (6) Brand, K. (1970) FEBS Lett., 7, 235-238.
- (7) Bais, R. and Keech, B. (1972) J. Biol. Chem., 247, 3255-3261.
- (8) Chen, Y-H, Yang, J. F., and Martinez, H. M. (1972) Biochemistry, 11, 4120-4131.
- (9) Morrison, J. F. and Uhr, M. L. (1966) Biochim. Biophys. Acta, 122, 57-74.
- (10) Daniel, E. and Weber, G. (1966) Biochemistry, 5, 1893-1900.
- (11) Frey, W. and Utter, M. F., personal communication.
- (12) Srere, P. A. (1969) in Methods in Enzymology, J. M. Lowenstein, ed., Vol. 13, pp. 3-11. Academic Press, New York.
- (13) Bock, R., Ling, N., Morell, S., and Lipton, S. (1956) Arch. Biochem. Biophys., 62, 253-264.
- (14) Scrutton, M. C. and Fung, C. H. (1972) Arch. Biochem. Biophys. 150, 636-647.
- (15) Kalckar, H. M. (1947) J. Biol. Chem., 167, 461-475.
- (16) Taylor, B. L., Barden, R. E., and Utter, M. F. (1972) J. Biol. Chem., 247, 7383-7390.

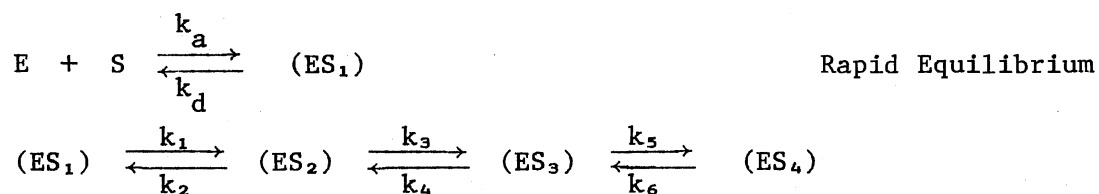
- (17) Robinson, H. W. and Hogden, C. G. (1940) J. Biol. Chem., 135, 707-725.
- (18) Cassim, J. Y. and Yang, J. T. (1969) Biochemistry, 8, 1947-1951.
- (19) Chandler, J. P. (1971) STEPIT, Quantum Chemistry Program Exchange, Indiana University Chemistry Department, Program 66.
- (20) Hamilton, W. C. (1969) Statistics in the Physical Sciences, Ronald Press Company, New York.
- (21) Bevington, P. R. (1969) Data Reduction and Error Analysis for the Physical Sciences, McGraw-Hill Book Company, New York.
- (22) Thompson, R. E. (1974) Ph.D. Dissertation, Oklahoma State University.
- (23) Secrist III, J. A., Barrio, J. R., Leonard, N. J., and Weber, G. (1972) Biochemistry, 11, 3500-3506.
- (24) North, F. C. and Spivey, H. O., personal communication.
- (25) Hill, D. E. (1972) Ph.D. Dissertation, Oklahoma State University.
- (26) Plowman, K. M. (1972) Enzyme Kinetics, McGraw-Hill Book Company, New York.
- (27) Cheung, H. C. and Morales, M. F. (1969) Biochemistry, 8, 2177-2182.
- (28) McClure, W. O. and Edelman, G. M. (1967) Biochemistry, 6, 559-566.
- (29) Kapoor, M. (1974) Can. J. Biochem., 32, 599-609.
- (30) Fan, C. C., Tomcho, L. A., and Plaut, G. W. (1974) J. Biol. Chem., 249, 5607-5613.
- (31) Dodd, G. H. and Radda, G. K. (1968) Biochem. J., 108P, 5-6.
- (32) Nakatani, H., Haga, M., and Hiromi, K. (1974) FEBS Lett., 43, 293-296.
- (33) Daniel, E. and Yang, J. F. (1973) Biochemistry, 12, 508-511.
- (34) Chen, Y-H, Yang, J. F., and Chau, K. H. (1974) Biochemistry, 13, 3350-3359.

APPENDIXES

APPENDIX A

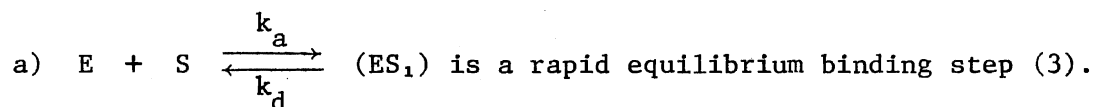
KINETIC TREATMENT OF MECHANISM PROPOSED FOR REACTION OF PYRUVATE CARBOXYLASE- ANS WITH MgATP

1. Proposed mechanism is



where E represents the pyruvate carboxylase-ANS complex, and S represents the substrate, MgATP. In the following treatment the last transition (conversion of (ES_3) to (ES_4)) has been uncoupled, since $\lambda_3 \gg \lambda_4$ (see Chapter III).

2. Assumptions



b) $[S] \approx [S_t]$ where $[S_t]$ is the initial MgATP concentration, since $[S] \gg [E]$ at all times. Thus the reaction is observed under conditions where $[S]$ is essentially constant.

3. Important auxiliary equations

a) Rapid Equilibrium Expression

$$K_f = \frac{k_a}{k_d} = \frac{[ES_1]}{[E][S_t]} \qquad (A-1)$$

where K_f is the equilibrium constant for the rapid equilibrium

step

b) Conservation Equation

$$[E_t] = [E] + [ES_1] + [ES_2] + [ES_3]$$

where $[E_t]$ is the total concentration of all enzyme containing species

4. Differential equations for the system

$$a) \frac{d[ES_1]}{dt} = k_a[E][S_t] - (k_d + k_1)[ES_1] + k_2[ES_2]$$

$$b) \frac{d[ES_2]}{dt} = k_1[ES_1] - (k_2 + k_3)[ES_2] + k_4[ES_3]$$

which reduce to

$$a) \frac{d[ES_1]}{dt} = -k_1[ES_1] + k_2[ES_2] \quad (A-2)$$

$$b) \frac{d[ES_2]}{dt} = (k_1 - (k_4/(K_f[S_t])) - k_4)[ES_1] - (k_2 + k_3 + k_4)[ES_2] + k_4[E_t] \\ = a'[ES_2] + b'[ES_1] + k_4[E_t] \quad (A-3)$$

where $a' = -(k_2 + k_3 + k_4)$ and

$$b' = (k_1 - (k_4/(K_f[S_t])) - k_4)$$

5. Let $[ES_1] = x$ and $[ES_2] = y$.

6. Solving the equations (A-2) and (A-3) simultaneously, the following solutions are obtained

$$a) x = c_1 e^{x_1 t} + c_2 e^{x_2 t} - \frac{k_2 k_4 [E_t]}{(a' k_1 + b' k_2)} \quad (A-4)$$

$$b) y = c_3 e^{x_1 t} + c_4 e^{x_2 t} - \frac{k_1 k_4 [E_t]}{(a' k_1 + b' k_2)} \quad (A-5)$$

where $c_1, c_2, c_3,$ and c_4 are constants to be obtained from initial conditions, and x_1 and x_2 are as follows:

$$\begin{aligned}
 x_1, x_2 = & \frac{1}{2}\{-(k_1 + k_2 + k_3 + k_4) \pm (k_1^2 + k_2^2 + k_3^2 + k_4^2 + 2k_1k_2 - \\
 & 2k_1k_3 - 2k_1k_4 + 2k_2k_3 - 2k_2k_4 + 2k_3k_4 - (4k_2k_4/(K_f[S_t])))^{1/2}\} \\
 = & \text{time constants, } -\lambda_2 \text{ and } -\lambda_3 \qquad \qquad \qquad \text{(A-6)}
 \end{aligned}$$

7. Assume that at the time of initial observation of the reaction (approximately 4 msec after mixing), (ES₁), E, and S have established an initial equilibrium; that is, the initial equilibrium establishment is unobserved. This assumption necessitates that the fluorescence emissivities of E and (ES₁) are approximately equal, since essentially no quenching occurs in the first 4 msec of unobserved reaction. From expression (A-1), at time $t \approx 0$

$$[ES_1]_0 = \frac{K_f[E_t][S_t]}{(1 + K_f[S_t])}$$

Time $t = 0$ will be taken as the time that reaction is observed so that $t \approx 0$ (4 msec) will be taken as $t = 0$. This assumption is based on a) If the bimolecular step were initially observed the ratio of initial slopes at 4.0 mM and 0.1 mM MgATP should be 40 at constant enzyme concentration; however, experimentally it is 2. b) Experimental values of λ_2 and λ_3 (and λ_4 for the coupled system) do not depend on MgATP concentration. c) Under conditions where the substrate is a "good" substrate (not a substrate analog), $t_{1/2}$ of the substrate binding step under conditions of 4 mM MgATP may be of the order of 10^{-6} sec. Based only on observations with other enzyme systems this last justification is not rigorous.

8. Determination of c_1 , c_2 , c_3 , and c_4

a) c_1 and c_2 are obtained under the following two initial conditions

$$1. \text{ At } t = 0, x = [ES_1]_0 = c_1 + c_2 - \frac{k_2 k_4 [E_t]}{(a'k_1 + b'k_2)}$$

from Equation (A-4)

$$2. \text{ At } t = 0, \frac{dx}{dt} = -k_1 [ES_1] = c_1 x_1 + c_2 x_2$$

from Equation (A-2) where $[ES_1]_0$ is the concentration of (ES_1) when reaction is observed at $t = 0$.

$$c_1 = \frac{1}{(x_2 - x_1)} \left\{ \frac{k_1 K_f [E_t] [S_t]}{1 + K_f [S_t]} + \frac{k_2 k_4 [E_t] x_1}{a'k_1 + b'k_2} + \frac{K_f [E_t] [S_t] x_1}{1 + K_f [S_t]} \right\} + \frac{k_2 k_4 [E_t]}{a'k_1 + b'k_2} + \frac{K_f [E_t] [S_t]}{1 + K_f [S_t]}$$

$$c_2 = \frac{1}{(x_2 - x_1)} \left\{ \frac{-k_1 K_f [E_t] [S_t]}{1 + K_f [S_t]} - \frac{k_2 k_4 [E_t] x_1}{a'k_1 + b'k_2} - \frac{K_f [E_t] [S_t] x_1}{1 + K_f [S_t]} \right\}$$

b) c_3 and c_4 are obtained under the following two initial conditions

$$1. \text{ At } t = 0, y = c_3 + c_4 - \frac{k_1 k_4 [E_t]}{(a'k_1 + b'k_2)} = 0$$

from Equation (A-5)

$$2. \text{ At } t = 0, \frac{dy}{dt} = b' [ES_1]_0 + k_4 [E_t]$$

from Equation (A-3)

$$c_3 = \frac{1}{(x_2 - x_1)} \left\{ \frac{k_1 k_4 [E_t] x_1}{a'k_1 + b'k_2} - \frac{k_1 K_f [E_t] [S_t]}{1 + K_f [S_t]} \right\} + \frac{k_1 k_4 [E_t]}{a'k_1 + b'k_2}$$

$$c_4 = \frac{1}{(x_2 - x_1)} \left\{ \frac{-k_1 k_4 [E_t] x_1}{a'k_1 + b'k_2} + \frac{k_1 K_f [E_t] [S_t]}{1 + K_f [S_t]} \right\}$$

9. The equations for all enzyme species are

$$a) [E] = \frac{[ES_1]}{K_f[S_t]} = \frac{c_1}{K_f[S_t]} e^{x_1 t} + \frac{c_2}{K_f[S_t]} e^{x_2 t} -$$

$$\frac{k_2 k_4 [E_t]}{K_f[S_t] (a'k_1 + b'k_2)}$$

$$b) [ES_1] = c_1 e^{x_1 t} + c_2 e^{x_2 t} - \frac{k_2 k_4 [E_t]}{(a'k_1 + b'k_2)}$$

$$c) [ES_2] = c_3 e^{x_1 t} + c_4 e^{x_2 t} - \frac{k_1 k_4 [E_t]}{(a'k_1 + b'k_2)}$$

$$d) [ES_3] = [E_t] - [E] - [ES_1] - [ES_2]$$

$$= c_5 e^{x_1 t} + c_6 e^{x_2 t} + c_7$$

$$\text{where } c_5 = \frac{-c_1}{K_f[S_t]} - c_1 - c_3$$

$$c_6 = \frac{-c_2}{K_f[S_t]} - c_2 - c_4$$

$$c_7 = [E_t] + \frac{k_2 k_4 [E_t]}{K_f[S_t] (a'k_1 + b'k_2)} + \frac{k_2 k_4 [E_t]}{(a'k_1 + b'k_2)}$$

$$+ \frac{k_1 k_4 [E_t]}{(a'k_1 + b'k_2)}$$

10. Derivation of final form

$$\frac{F_0 - F_t}{F_0} = \frac{\epsilon_0 [E]_0 - \epsilon_0 [ES_1]_0 - \epsilon_0 [E] - \epsilon_1 [ES_1]}{\epsilon_0 [E]_0 + \epsilon_0 [ES_1]_0}$$

$$- \frac{\epsilon_2 [ES_2] + \epsilon_3 [ES_3]}{\epsilon_0 [E]_0 + \epsilon_0 [ES_1]_0}$$

$$= 1 - \left\{ \frac{c_8 e^{x_1 t} + c_9 e^{x_2 t} + c_{10}}{\epsilon_0 [E_t]} \right\} \quad (\text{A-6})$$

where F_0 and F_t are fluorescence at initial time and time, t , respectively, and ϵ_0 , ϵ_2 , ϵ_3 are fluorescence emissivities of E and (ES_1) , (ES_2) , and (ES_3) , respectively and

$$c_8 = \frac{\epsilon_0 c_1}{K_f [S_t]} + \epsilon_0 c_1 + \epsilon_2 c_3 + \epsilon_3 \left\{ \frac{-c_1}{K_f [S_t]} - c_1 - c_3 \right\}$$

$$c_9 = \frac{\epsilon_0 c_2}{K_f [S_t]} + \epsilon_0 c_2 + \epsilon_2 c_4 + \epsilon_3 \left\{ \frac{-c_2}{K_f [S_t]} - c_2 - c_4 \right\}$$

$$c_{10} = \epsilon_0 \left\{ \frac{-k_2 k_4 [E_t]}{K_f [S_t] (a'k_1 + b'k_2)} - \frac{k_2 k_4 [E_t]}{a'k_1 + b'k_2} \right\} +$$

$$\epsilon_2 \left\{ \frac{-k_1 k_4 [E_t]}{a'k_1 + b'k_2} \right\} + \epsilon_3 \left\{ [E_t] + \frac{k_2 k_4 [E_t]}{K_f [S_t] (a'k_1 + b'k_2)} + \right.$$

$$\left. \frac{k_2 k_4 [E_t]}{a'k_1 + b'k_2} + \frac{k_1 k_4 [E_t]}{a'k_1 + b'k_2} \right\}$$

Equation (A-6) reduces to

$$\frac{F_0 - F_t}{F_0} = B - (A2)e^{x_1 t} - (A3)e^{x_2 t}$$

$$\text{where } B = 1 - \frac{c_{10}}{\epsilon_0 [E_t]}$$

$$A2 = \frac{c_8}{\epsilon_0 [E_t]}$$

$$A3 = \frac{c_9}{\epsilon_0 [E_t]}$$

$$-\lambda_2 = x_1 \quad \text{and} \quad -\lambda_3 = x_2$$

Since (A2) + (A3) = B,

$$\frac{F_0 - F_t}{F_0} = A_2 + A_3 - (A_2)e^{-\lambda_2 t} - (A_3)e^{-\lambda_3 t} \quad (\text{A-7})$$

11. Observations

- a) A2 and A3 have no $[E_t]$ dependence. Every term in c_8 , c_9 , and c_{10} from which B, A2, and A3 are obtained contain a $[E_t]$ term in the numerator. When c_8 , c_9 , and c_{10} are divided by $\epsilon_0[E_t]$, the $[E_t]$ dependence cancels.
- b) λ_2 and λ_3 have one term with dependence on MgATP concentration.
- c) The amplitude (pre-exponential) parameters are sums and differences of three types of terms

1) Type 1: $\frac{a_1 K_f [S_t]}{1 + K_f [S_t]}$ where a_1 is a constant. This is

a rectangular hyperbola dependence on substrate concentration.

2) Type 2: $\frac{b_1}{a'k_1 + b'k_2}$ where b_1 is a constant, which

reduces to $\frac{b_2 K_f [S_t]}{1 + b_3 K_f [S_t]}$ where b_2 and b_3 are constants.

This is a rectangular hyperbola dependence on substrate concentration.

3) Type 3: $\frac{a_1 K_f [S_t]}{K_f [S_t] (1 + K_f [S_t])}$ and $\frac{b_1}{K_f [S_t] (a'k_1 + b'k_2)}$

which reduce to $\frac{a_1}{1 + K_f [S_t]}$ and $\frac{b_2}{1 + b_3 K_f [S_t]}$

respectively, where a_1 , b_1 , b_2 , and b_3 are constants. This is not a rectangular hyperbola dependence on substrate concentration.

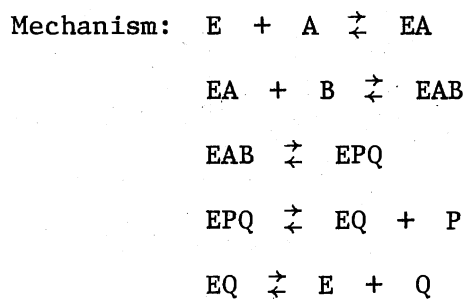
APPENDIX B

NOMENCLATURE FOR ENZYME MECHANISMS

The following is a summary of the nomenclature proposed by W. W. Cleland (4) to describe mechanisms for enzyme-catalyzed reactions. Primarily, nomenclature directly pertinent to this thesis is included.

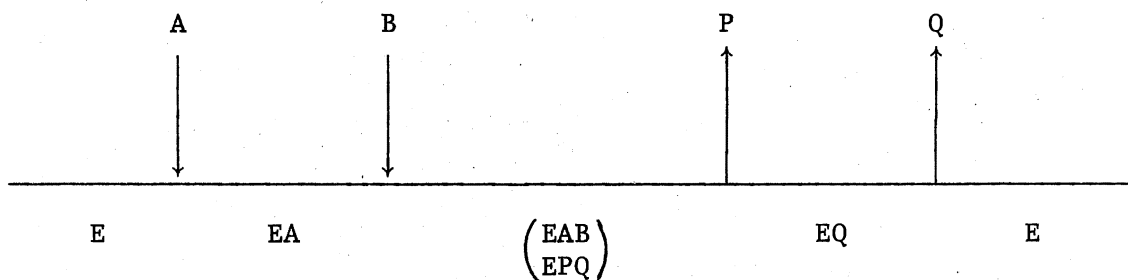
- 1) The number of kinetically important substrates or products in a mechanism is designated by the syllables Uni, Bi, Ter, and Quad. Thus a reaction with two substrates and two products is designated Bi Bi.
- 2) The order of addition of substrates and release of products within the reaction sequence is described as follows. Mechanisms where all substrates must add to the enzyme before any products are released are designated "sequential." Such mechanisms are called "Ordered" if the substrates add in obligatory order and the products leave similarly, and "Random" if the substrates do not react in obligatory order and alternate reaction sequences exist. When one or more products are released before all substrates have added to the enzyme, the enzyme exists in two or more stable forms between which it oscillates during the reaction. Such reactions are called "Ping Pong," and if the mechanism is not obvious it is further described by use of Uni, Bi, and Ter, to indicate the successive groups of substrate additions and product dissociations that occur.

- 3) For graphical presentation the reaction sequence is written from left to right in a repeating sequence. The enzyme is represented by a horizontal line, and substrate additions and product dissociations are represented by vertical arrows. Substrates, products, and enzyme forms are labeled for clarity and identification. For example, the following mechanism is graphically represented as shown below.



where E is the enzyme, A and B are substrates, and P and Q are products.

Graphical representation:



VITA

Karen Sue Reinschmiedt McGurk

Candidate for the Degree of

Doctor of Philosophy

Thesis: I. EFFECTS OF ADENINE NUCLEOTIDES ON THE CATALYTIC ACTIVITY OF MITOCHONDRIAL PORCINE HEART MALATE DEHYDROGENASE
II. LIGAND INDUCED CONFORMATIONAL TRANSITIONS AND SECONDARY STRUCTURE COMPONENTS OF CHICKEN LIVER PYRUVATE CARBOXYLASE

Major Field: Chemistry

Biographical:

Personal Data: Born in Elk City, Oklahoma, November 14, 1949, the daughter of John J. and Lillian R. Reinschmiedt.

Educational: Graduated from Clinton High School, Clinton, Oklahoma, in 1968; received the Bachelor of Science degree in Chemistry (summa cum laude) from Southwestern Oklahoma State University, Weatherford, Oklahoma, in 1972; completed requirements for the Doctor of Philosophy degree on May 8, 1976.

Professional Experience: Served as an undergraduate research participant in the summer of 1972 at Argonne National Laboratory at Argonne, Illinois; served as NSF Fellow, 1972-1973; served as American Cancer Society graduate research assistant at Oklahoma State University, 1973-1974; served as graduate research assistant in biochemistry at Oklahoma State University, 1974-1976.

Professional Organizations: Member of the Society of Sigma Xi.